Ultrathin Films and Supramolecular Architecture of Phthalocyanine Derivatives

藤木, 道也

https://doi.org/10.11501/3065641

出版情報：九州大学, 1992, 博士（工学）, 論文博士
バージョン：
権利関係：

CHAPTER 4

DIRECT PATTERNING AND ELECTRICAL PROPERTIES OF ALKYLAMIDE SUBSTITUTED PHTHALOCYANINE THIN FILMS

SYNOPSIS

Patterning and electrical properties of thin films based on soluble nickel phthalocyanines with four long alkyl amides (AmPc1 and AmPc2) are examined. The films are prepared by the Langmuir-Blodgett and spin cast techniques. The film conductivities increase by 2 - 4 orders of magnitude upon iodine vapor exposure up to the value of ca. 10^{-6} $S \cdot cm^{-1}$. Both AmPc1 and AmPc2 thin films show negative patterning features to electron beam (EB) dose, and excellent resistance to plasma assisted dry etching. AmPc2 possesses a high contrast value in the LB film ($\gamma = 3.8$) and a high reactivity ($D_0 = 3.5$ $\mu C \cdot cm^{-2}$) in the spin cast film. The fine patterns in AmPc2 spin cast film have been fabricated down to lines of width 0.8 μm with 0.8 μm spacing using EB irradiation and wet etching, probably without losing the semiconducting properties of the Pc ring moieties without decomposition.

§4-1. Introduction

Because thin film of phthalocyanines (Pc's) exhibits several unique photonic and electronic properties, many studies have continued for potential applications, such as solar cells,[1,2] photosensitizers,[3-5] gas sensors,[5,6] and electrochromisms.[8] Thin films of unsubstituted Pc's can be frequently obtained by vacuum deposition and dispersion in a polymer binder, due to extremely poor solubilities in organic solvents. Since the successful study on the Langmuir-Blodgett (LB) film of substituted Pc's, a number of reports have appeared on the preparation, characterization, and electrical properties of the LB films using soluble Pc's containing short and long alkyl moieties.[9-18]

In Chapters 2 and 3, it has been revealed that two soluble nickel phthalocyanines with four long chain alkyl amides (AmPc1 and AmPc2), form good quality LB films exhibiting one-dimensional self-assembled structures. If fine patterns of photonic and electrical active Pc LB films are directly formed by lithography without losing their functionalities, the films should display many advantages, such as prevention of ionic contamination or saving of the patterning processes.

Although there are several lithography studies on LB films of long chain alkyl carboxylic acids and esters, only limited works have been attempted on functionalized organic thin films.[19-21] For examples, one μm test patterns of polydiacetylene LB films have bee reported for non-linear optical waveguides using UV lithography.[22] Ten nm patterns

Table 4-1. In-Plane Conductivities of AmPc1 and AmPc2 Thin Films.

	AmPc1		AmPc2	
	LB[a)]	Spin Cast	LB[b)]	Spin Cast
	$S \cdot cm^{-1}$	$S \cdot cm^{-1}$	$S \cdot cm^{-1}$	$S \cdot cm^{-1}$
Undoped	$(0.8\text{-}8) \cdot 10^{-10}$	$(0.4\text{-}2) \cdot 10^{-10}$	$(4\text{-}7) \cdot 10^{-8}$	$(0.5\text{-}2) \cdot 10^{-9}$
I_2 doped	$(0.8\text{-}2) \cdot 10^{-6}$	$(2\text{-}4) \cdot 10^{-7}$	$(0.7\text{-}2) \cdot 10^{-6}$	$(2\text{-}8) \cdot 10^{-7}$

[a] Y-type LB film prepared by the vertical dipping method, 20 layers (= 700Å thickness). [b] spin cast film, 0.2 μm thickness. [c] X-type LB film prepared by the horizontal lifting method, 10 layers (= 370 Å thickness).

of manganese stearate LB films have been demonstrated using electron beam (EB) lithography in relation to low-dimensional magnetism.[23] Thirty μm pitch patterns of conducting polypyrrole formed by electrochemical polymerization have been fabricated on insulating polymer films.[24]

In this chapter, we will demonstrate direct fine patterning properties in relation to EB dose, plasma assisted dry etching durability, and electrical properties of LB and spin cast films of AmPc1 and AmPc2 toward application of phthalocyanine thin films.

§4-2. Electrical Conductivity

Table 4-1 summarizes the in-plane conductivities of AmPc1 and AmPc2 thin films at room temperature. In both of the undoped and I_2 doped state, dark conductivities in the LB films are higher than those in the spin cast films by one order of magnitude. This suggests that the conducting paths in the LB film are in ordered states compared with those in the spin cast film. When the undoped LB and spin cast films are exposed with I_2 vapor, the conductivities increase by about four orders of magnitude for AmPc1 and by about two orders of magnitude for AmPc2. The film conductivity reach about 10^{-6} $S \cdot cm^{-1}$ in all cases. These conductivities, however, are extremely low by five to six orders of magnitude in comparison with previously reported values for unsubstituted Pc-iodine charge-transfer complexes.[28,29] This diference may arise from both the imperfection of conducting paths in film plane and the presence of bulky and insulating long alkyl chain units of AmPc1 and AmPc2.

Figure 4-1 shows the change in the conductivity of AmPc1 and AmPc2 LB films as a function of the I_2 vapor exposure time. The time dependence of the conductivity in AmPc1 differs markedly from that in AmPc2, though both of them finally attain ca. 10^{-6} $S \cdot cm^{-1}$. The conductivity of AmPc2 reaches a constant value within 1 min, while AmPc1 requires 0.5 - 1 hr. Such difference in the response curves can be attributed to the fact that AmPc2, which includes electron donating amides, is more sensitive to I_2 oxidation than AmPc1, which has electron accepting amides.[30]

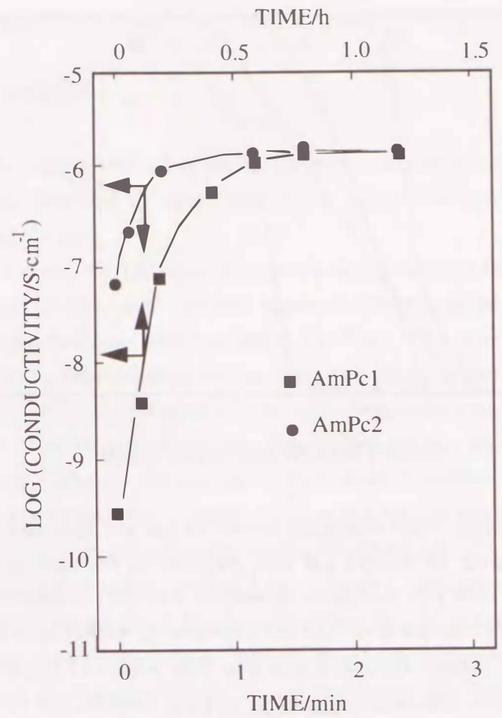

Figure 4-1. In-plane dark conductivities of AmPc1 and AmPc2 LB films as a function of exposure time to iodine vapor in a sealed box at room temperature (AmPc1: 20 layers, AmPc2: 10 layers, maximum vapor pressure of iodine ca. 0.3 mmHg).

§4-3. Patterning Properties of the Phthalocyanine Thin Films

Patterning properties of films were evaluated as follows. EB exposure was carried out using a computer-controlled EB writing machine (Elionix ELS-5000, with an accelerating voltage of 20 kV), after pre-baking at 100 ˚C for 20 min. The exposed samples were then developed by immersing them in developing solvents and rinsing in a non-solvent. Dry etching durability was evaluated from the remaining fractional thickness, using a reactive ion sputtering etching apparatus (Anelva DEM451 RIE). The normarized reactivity with negative character (R) and contrast (γ) are given as follows:

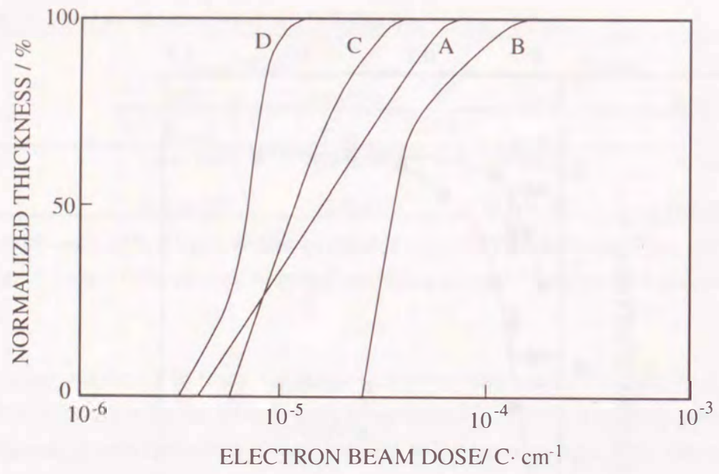

Figure 4-2. Electron beam sensitivity curves of LB and spin cast films of AmPc1 and AmPc2. (A:AmPc1 LB film prepared by the vertical dipping technique with 0.08 μm thickness, B:AmPc2 LB film prepared by the horizontal lifting technique with 0.18 μm thickness, C:AmPc1 spin cast film with 0.11 μm thickness, D:AmPc2 spin cast film with 0.13 μm thickness, developing solvents: $CHCl_3/CH_3OH$ = 6/1, 15 s and CH_3OH, 30s for AmPc1 and $CHCl_3/CH_3OH$ = 4/1, 15 s and CH_3OH, 30 s for AmPc2).

Table 4-2. Patterning Characteristics by Electron Beam Dose of AmPc1, AmPc2, and Other Polymeric Negative Resists.

Material	Film state	D_0[a)]	R[a)]	γ[a)]	ref
		$\mu C \cdot cm^{-2}$	$mg \cdot C \cdot cm^{-2}\ mol^{-1}$		
AmPc1[b)]	LB[f)]	4.3	7	0.9	this work
	Spin cast	5.6	10	1.7	this work
AmPc2[c)]	LB[g)]	26	47	3.8	this work
	Spin cast	3.5	6.3	1.6	25
CMS[d)]	Spin cast	1.3	130	1.8	31
PGMA[e)]	Spin cast	0.22	28	2.0	32

[a] D_0, R, γ mean the sensitivity, reactivity, and contrast, respectively. [b] developing solvent: $CHCl_3/CH_3OH$ = 6/1 (15 s) and CH_3OH (30 s). [c] developing solvent: $CHCl_3/CH_3OH$ =4/1 (15 s) and CH_3OH (30s). [d] M_w: $1.0 \cdot 10^5$. [e] M_w: $1.25 \cdot 10^5$. [f] 70 layers, Y-type film. [g] 39 layers, X-type films.

$$R = D_0 \cdot M_w \quad (4\text{-}1)$$

$$\gamma = 1/[2 \cdot \log(D_{50}/D_0)] \quad (4\text{-}2)$$

where D_0 is EB sensitivity defined as the minimum dose required to form an insoluble gel on the substrate, D_{50} is a dose to remain half of the initial thickness, and M_w is molecular weight of the material used.

Figure 4-2 shows the EB sensitivity curves of LB and spin cast films of AmPc1 and AmPc2. Both AmPc1 and AmPc2 possess negative patterning properties in which the films remain at the initial thickness with increasing EB dose. This indicates that cross-linking reactions occur during EB irradiation and insoluble gels are generated in the thin film.

Table 4-2 summarizes the sensitivities, reactivities, and contrasts for AmPc1, AmPc2, and other typical negative polymer resists. The AmPc2 LB film shows the highest contrast value among these materials. Except for AmPc2 LB film, AmPc1 and AmPc2 in the thin films are 13-20 times more reactive than chloromethylated polystyrene (CMS)[31] and 3 - 4 times more reactive than poly(grycidyl methacrylate) (PGMA).[32] The reactivities of the films are in the following order: AmPc2 LB << AmPc1 spin cast < AmPc1 LB < AmPc2 spin cast. The contrast values of the Pc films are in the following order: AmPc2 LB > AmPc1 spin cast > AmPc2 spin cast > AmPc1 LB. These results mean that the order of the reactivity is almost the reverse of that of the contrast value. Such an inverse relation might be related to the state of entanglement of the Pc moieties.

Figure 4-3 illustrates proposed entanglement models. The amide units of the Pc molecules can effectively interact with each other through the hydrogen-bonding force in the spin cast and in the Y-type LB film layers. In contrast, the amide units of the Pc molecules in the X-type LB film limits the hydrogen-bonding interaction between film layers. This effect results in an apparent decrease in the molecular weight of the Pc aggregates and leads to a decrease of reactivity and an increase of contrast. This explanation is consistent with the well-known fact that negative polymer resists give increasing reactivity values and decreasing contrast values with an increase in the molecular weight of materials.[31]

§4-4. Cross-Linking Reaction Mechanism

Both of AmPc1 and AmPc2 do not seem to have efficient cross-linking sites similar to the chloromethyl group in CMS and epoxy group in PGMA, though AmPc1 and AmPc2 have much higher reactivities than CMS and PGMA. CMS causes a cross-linking between polymer chains through dissociation of the C-Cl bonding in the chloromethyl group. PGMA forms an insoluble gel through the ring opening chain reaction of the more reactive epoxy C-O-C group.

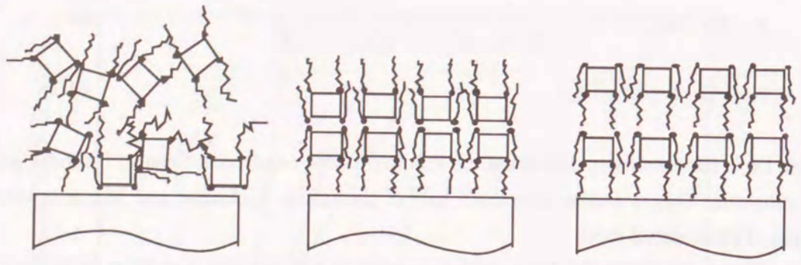

Figure 4-3. Proposed entanglement models of AmPc1 and AmPc2 molecules in the spin cast, X-type and Y-type LB films (square, circle, solid line represent Pc ring, amide, alkyl chain, respectively).

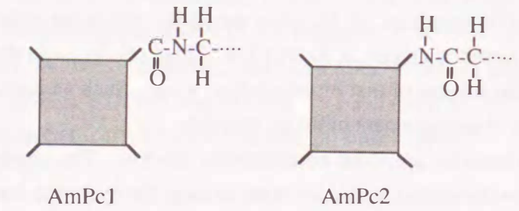

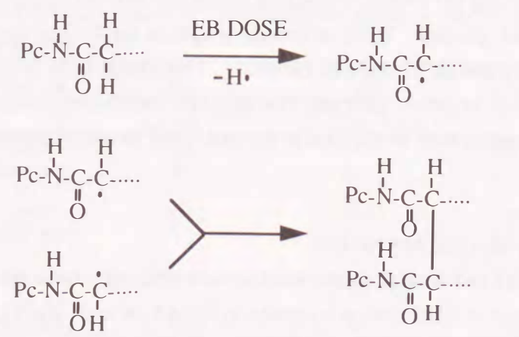

Figure 4-4. Possible cross-linking schemes of AmPc1 and AmPc2 under electron beam irradiation.

Table 4-3. Dry Etching Durabilities in AmPc1, AmPc2, and other Materials (Å/min).

Etching gases	Material				Etching Condition	
	AmPc1[a)]	AmPc2[a)]	Novolac[a)b)]	Si[c)]	Pressure (Pa)	RF power (W/cm^2)
$CBrF_3$	<25	<25	230	530	13	0.32
CF_4 + 4% O_2	1050		1150		80	0.30
O_2	470		750		13	0.10

[a] Spin cast films. [b] Shipley, AZ-1350J. [c] Wafer.

In order to clarify such situations, the reaction process was examined under an Ar gas atmosphere for 3 hr (4.9 W at 185 nm and 24.4 W at 254 nm) by means of visible and FT-IR spectroscopies. AmPc1 and AmPc2 became insoluble during UV exposure and EB irradiation. This is because secondary electrons from the underlying substrate under EB irradiation cause cross-linking of the most reactive or weak bonding sites in the same manner as occurs during UV irradiation. Unfortunately, spectral changes of AmPc1 and AmPc2 in visible and IR region were not recognized after UV irradiation. This indicates that after UV irradiation no Pc rings are decomposed and no alkyl amide moieties are dissociated and denatured. Pc rings in AmPc1 and AmPc2 are not expected to decompose by EB dose, since Pc rings are 10^2 - 10^4 times more stable to EB irradiation than aliphatic compounds.[33]

Adjacent a(C-H) bonding of the amide group is considered to become the reactive site in the Pc molecules. Unfortunately, no dissociation energy from the adjacent C-H bonding of the amides has been observed, while dissociation energies are reported to be 68 kcal/mol for the $PhCH_2$-Cl bonding as the active site of CMS and 51 kcal/mol for the C-O-C bonding as the active site of PGMA.[34] Nylon 66, which includes aliphatic amides, has been reported that chain decomposition mainly occurs compared to chain cross-linking during g-ray irradiation.[35] Nevertheless, since AmPc1 and AmPc2 are aromatic amide compounds exhibiting large resonance stabilization and polarization energies,[36] the adjacent C-H bondings of the amide units may lead to dissociation and cross-linking.

Figure 4-4 displays the possible cross-linking schemes by EB dose for AmPc1 and AmPc2. In the first step, the adjacent C-H bonding produces secondary alkyl radicals under irradiation. Next, the radical couples with neighboring radicals and produces cross-linking. Finally, *tert*-alkyl moieties are formed. As is well-known, the C-H bonding stretching intensity in *tert*-alkyl group is much weaker than those in the secondary and primary alkyl groups. Such *tert*-alkyl part is also a very small fraction among the C-H bonding units. Hence, no detectable changes in the C-H stretching region are detected even using FT-IR spectroscopy.

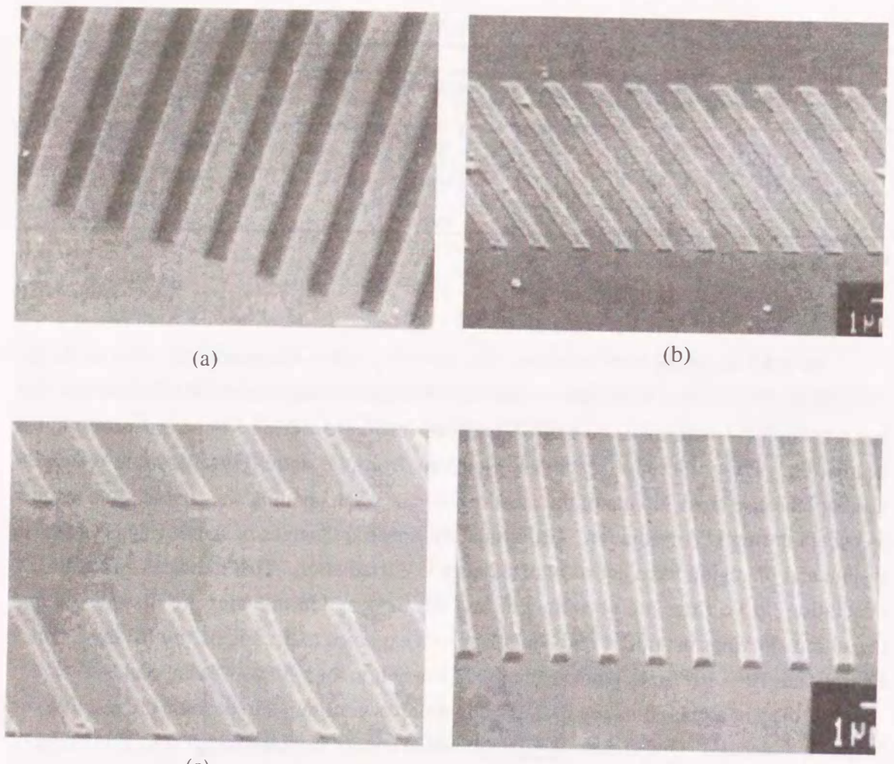

(a) (b)

(c) (d)

Figure 4-5. Scanning electron micrographs of fine patterns in AmPc1 and AmPc2 thin films on silicon wafer using EB irradiation and wet etching. (a:AmPc1 LB film prepared by the vertical dipping method, 9 μm lines and 16 μm spaces, b:AmPc1 spin cast film, 1 μm lines and 1 μm spaces, c:AmPc2 LB film prepared by the horizontal lifting method, 1 μm lines and 3 μm spaces, d:AmPc2 spin cast film, 0.8 μm lines and 0.8 μm spaces).

§4-5. Dry Etching Durability

The plasma assisted dry etching process has been recently noted as an alternative pattern delineation process better than the wet etching process. Table 4-3 gives the etching rates in AmPc1, AmPc2, and other materials to a variety of etching gases. In $CBrF_3$ plasma gas conditions the etching rates in AmPc1 and AmPc2 are one tenth of the novolac resin which is a typical dry etching durable polymer,[37,38] and one twentieth of silicon wafer, while the rates of the Pc's are comparable to that of the resin under condition of CF_4-4% O_2 and O_2 plasma gasses. Such excellent dry-etching durabilities of AmPc1 and AmPc2 originate from

the inherent large polarizability and resonance energies of the Pc ring,[36] since dry etching durabilities of negative resists are recognized to increase with increases in the resonance energies of the materials.[38]

Under $CBrF_3$ plasma gas condition, only milder active species such as $\cdot CF_3$ and $\cdot Br$ would be generated instead of highly active species such as $\cdot F$ and $\cdot O$, as shown above. Such milder active species would result in selective etching characteristics instead of a decrease in the etching rate of the organic and inorganic substances. This is consistent with the experimental results listed in Table 4-4.

When a large electric field is applied to etching gasses, various active species are believed to generate in the following scheme:[19]

$$2\,e + 2\,CF_4 \longrightarrow \cdot CF_3 + :CF_2 + 3\cdot F + 2e \quad (4\text{-}3)$$

$$e + O_2 \longrightarrow 2\cdot O + e \quad (4\text{-}4)$$

$$\cdot O + :CF_2 \longrightarrow \cdot COF_{2-x} + x\cdot F \quad (4\text{-}5)$$

$$e + CBrF_3 \longrightarrow \cdot CF_3 + \cdot Br + e \quad (4\text{-}6)$$

§4-6. Fine Patterns Using Electron Beam Lithography

Figure 4-5(a)-(d) shows scanning electron micrographs of fine patterns in LB and spin cast films of AmPc1 and AmPc2 using EB irradiation and wet etching. The AmPc2 in LB film can be delineated down to 1 μm lines and 3 μm spaces because of its high contrast value. AmPc1 in LB film can be delineated to only 9 μm lines and 16 μm spaces due to its low contrast value. The fine patterns in spin cast films can be obtained down to 1.0 μm lines and 1.0 μm spaces for AmPc1 and 0.8 μm lines and 0.8 μm spaces for AmPc2, respectively. These photographs indicate that fine patterns in semiconducting Pc thin films can be formed directly using EB lithography, while maintaining their electrical activities without decomposition of Pc rings.

§4-7. Preparation of the Phthalocyanine Thin Films

Spin cast films were prepared from 10^{-1} M $CHCl_3$ solutions of AmPc1 or AmPc2. Multilayer films of AmPc1 and AmPc2 were deposited at 20 $mN \cdot m^{-1}$ of film pressure by the vertically dipping and horizontally lifting methods, as described in Chapter 3. Optically polished hydrophobic quartz and silicon wafer were obtained by treating with a silane coupling agent for patterning and electrical measurements. The film thickness deposited was determined by a mechanical stylus method (Taylor-Hobson Talystep or Kosaka model ET-10).

§4-8. Conclusion

The patterning and electrical properties of thin films of two new highly soluble nickel phthalocyanines with long chain alkyl amides (AmPc1 and AmPc2) have been examined. The films have been prepared by the LB and spin cast technique.

The dark conductivities of the films increase by two to four orders of magnitude upon iodine vapor exposure and attain σ = ca. 10^{-6} S·cm^{-1}. Such extremely low conductivity is believed to result from the presence of the insulating long chain alkyl moieties of AmPc1 and AmPc2.

AmPc1 and AmPc2 thin films show negative patterning properties to electron beam (EB) dose. The AmPc2 LB films exhibits high contrast value as high as $\gamma = 3.8$. The AmPc2 spin cast film also shows high reactivity as small as $D_0 = 3.5$ μC·cm^{-2}. Such high reactivity and contrast values are conceivably related to the hydrogen-bonding interaction and adjacent C-H bonding of the amide units in the Pc molecules. This is based on the fact that no spectral changes in visible and IR region for AmPc1 and AmPc2 thin films are observed after UV irradiation.

Plasma-assisted dry etching durabilities of AmPc1 and AmPc2 are 1 - 10 times higher than that of the novolac resin, which is a typical dry etching durable polymer resist. This arises from the inherent large resonance and polarization energies of Pc rings. The fine patterns in AmPc2 spin cast films have been fabricated down to 0.8 μm lines and 0.8 μm spaces using EB irradiation and wet etching, without losing the semiconducting properties of Pc ring moieties without decomposition.

§4-9 References

1. Loutfy, R. O.; Sharp, J. H. *J. Chem. Phys.* **1979**, *71*, 1211.
2. Tang, C. W. *Appl. Phys. Lett.* **1982**, *40*, 183.
3. Arishima, K.; Hiratsuka, H.; Tate, A.; Okada, T. *Appl. Phys. Lett.* **1985**, *46*, 279.
4. Kato, M.; Nishioka, Y.; Kaifu, K.; Kawamura, K.; Ohno, S. *Appl. Phys. Lett.* **1985**, *46*, 196.
5. Loutfy, R. O.; Hor, A. M.; DiPaola-Baranyi, G.; Hsiao, C. K. *J. Imag. Sci.* **1985**, *29*, 116.
6. Honeybourne, C. L.; Ewen, R. J.; Hill, C. A. S. *J. Chem. Soc. Faraday Trans. 1.* **1984**, *80*, 851.
7. Moskalev, P. N.; Kirin, I. S. *Russ. J. Phys. Chem.* **1972**, *46*, 1019.
8. Yamamoto, H.; Sugiyama, T.; Tanaka, M. *Jpn. J. Appl. Phys.* **1985**, *24*, L305.
9. Carter, F. L., Ed. *Molecular Electronic Devices* ; Dekker, New York, NY, 1982.
10. *Thin Solid Films* **1983**, 99, 1.
11. Barlow:, W. A., Ed. *Langmuir-Blodgett Films* ; Elsevier, Amsterdam, Netherland, 1980.

12. *Thin Solid Films* **1985**, Vol. 132-134.
13. Hann, R. A.; Gupta, S. K.; Fryer, J. R.; Eyres, B. L. *Thin Solid Films* **1985**, *134*, 35.
14. Kovacs, G. J.; Vincett, P. S.; Sharp, J. H. *Can. J. Phys.* **1985**, *63*, 346.
15. Roberts, G. G.; Petty, M. C.; Baker, S.; Fowler, M. T.; Thomas, N. J. *Thin Solid Films* **1985**, *132*, 113.
16. Barger, W. R.; Snow, A. W.; Wohltjen, H.; Jarvis, N. L. *Thin Solid Films* **1985**, *133*, 197.
17. Kalina, D. W.; Crane, S. W. *Thin Solid Films* **1985**, *134*, 109.
18. Yoneyama, M.; Sugi, M.; Saito, M.; Ikegami, K.; Kuroda, S.; Iizima, S. *Jpn. J. Appl. Phys.* **1986**, *25*, 961.
19. Thompson, L. F.; Wilson, C. G.; Bowden:, M. J. *Introduction to Microlithography* ; ACS, Washington, DC., 1983.
20. A. Ledwith, A. *IEE. Proc. 1. Solid State and Electron Devices* **1983**, *130*, 245.
21. Peterson, I. R. *IEE. Proc. 1. Solid State and Electron Devices* **1983**, *130*, 252.
22. Williams, D. J., Ed. *Nonlinear Optical Properties of Organic and Polymeric Materials* ; ACS: Washington, DC, Garito, A. F.; Singer, K. D.; Teng, C. C. Chap. 1, 1983.
23. Broers, A. N.; Pomerantz, M. *Thin Solid Films* **1983**, *99*, 323.
24. Hikita, M.; Niwa, O.; Sugita, A.; Tamamura, T. *Jpn. J. Appl. Phys.* **1985**, *24*, L79.
25. Tabei, H.; Fujiki, M.; Imamura, S. *Jpn. J. Appl. Phys.* **1985**, *24*, L685.
26. Shirai, H.; Maruyama, A.; Kobayashi, K.; Hojo, N. Mackomol. Chem. **1980**, *181*, 575.
27. Nakahara, H.; Fukuda, K. *J. Colloid Interface Sci.* **1979**, *69*, 24.
28. Peterson, J. L.; Schramn, C. S.; Stojakovic, D. R.; Hoffman, B. M.; Marks, T. J. *J. Am. Chem. Soc.* **1977**, *99*, 286.
29. Blant, P.; Weber, D. C.; Haupt, S. G.; Nohr, R. S.; Wynne, K. J. *J. Chem. Soc. Dalton Trans.* **1985**, 269.
30. Furguson, L. N. *The Modern Structural Theory of Organic Chemistry* ; Prentice-Hall, Englewood Cliffs, NJ., 1963.
31. Imamura, S.; Tamamura, T; Harada, K.; Sugawara, S. *J. Appl. Polym. Sci.* **1982**, *27*, 937.
32. Taniguchi, Y.; Hatano, Y.; Shiraishi, H.; Horigome, S.; Nonogaki, S.; Naraoka, K. *Jpn. J. Appl. Phys.* **1979**, *18*, 1143.
33. Ueda, N. *Dyes and Pigments*, **1985**, *6*, 115.
34. Kagiya, T. *Kagakuhanno no Sokudoronteki Kenkyuhou*; Kagaku Dojin, Kyoto, Japan, Appendix, 1970.
35. Dole, M. *The Radiation Chemistry of Macromolecules* ; Academic, New York, NY, Vol. 2, Chap. 7., 1973.

36. Xian, C. S.; Seki, K.; Inokuchi, H.; Zurong, S.; Renyuan, Q. *Bull. Chem. Soc. Jpn.* **1983**, *56*, 2565.
37. Lehman, H. W.; Widmer, R. *Appl. Phys. Lett.* **1978**, *32*, 163.
38. Imamura, S.; Tamamura, T.; Kogure, O. *Polymer J.* **1984**, *16*, 391.

CHAPTER 5

FACILE SYNTHESES OF SOLUBLE PHTHALOCYANINES WITH SHORT ALKYL SUBSTITUENTS

SYNOPSIS

Several tetra(*tert*-butyl)phthalocyanine derivatives can be prepared from the corresponding alkylbenzenes in two or three steps, while a previously method required seven steps from *o*-xylene. The facile short step synthesis conducts a preparation of two new types of copper phthalocyanines that contain both alkyl (*tert*-butyl or *iso*-propyl) and cyano groups from the corresponding alkylbenzenes in only two steps with excellent yields. ^{1}H NMR spectra and high performance liquid chromatogram indicated the presence of three of four possible geometric isomers of tetra(*tert*-butyl)phthalocyanines. Reaction mechanisms of these preparative processes are also discussed.

§5-1. Introduction

Soluble phthalocyanines (Pc's) have received much attention because of their photonic and electronic devices.[1-8] Since it is known that the Langmuir-Blodgett (LB) technique is applicable to prepare ultrathin films of soluble Pc's, several workers have studied on the preparation, structure and electrical properties of LB films of highly soluble tetra(*tert*-butyl)metallophthalocyanine (M(TBP), M represents central metal ion).[9-11] Unfortunately, subtle control of the preparative condition, such as spreading solvents, additives in the subphase, subphase temperature, and concentration of TBP molecule, is necessary in order to obtain reproducibly their high-quality LB films. In addition, the previously reported method requires seven steps from *o*-xylene to obtain M(TBP) derivatives.[12-14]

In Chapters 2 to 4, we demonstrated that the Pc's substituted with four long alkyl secondary amides self-assembled to one-dimensionally stacked structures in the solid, in the cast film, and even in the solution, due to the strong, intermolecular hydrogen-bonding. At the same time, an introduction of long alkyl moieties facilitated formation of LB films with one-dimensional Pc array and fixed orientations. However, the existence of electrically insulating long alkyl moieties seems to prevent continuous transport of hole carrier when the Pc LB films are exposed to iodine vapor, as indicated from their low conductivities.

As a second attempt to improve LB film formation and the doping effect, two types of Cu^{II} (tetracyanophthalocyanine) with four short alkyl substituents (*tert*-butyl or *iso*-propyl) were designed based on the following considerations. If four hydrophilic cyano units are symmetrically introduced on the Pc ring, they can afford LB film forming ability to the Pc

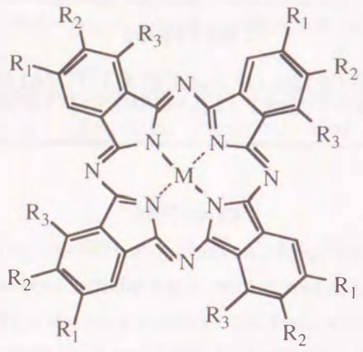

ABBREVIATION	M	R_1	R_2	R_3
Ni(TBP)	Ni	*tert*-butyl	H	H
Cu(TBP)	Cu	*tert*-butyl	H	H
Pb(TBP)	Pb	*tert*-butyl	H	H
H_2(TBP)	H_2	*tert*-butyl	H	H
Cu(TBCP)	Cu	*tert*-butyl	H	CN
Cu(IPCP)	Cu	*iso*-propyl	CN	H

Figure 5-1. Lightly substituted phthalocyanine derivatives prepared in this work.

molecule and increase both of electron affinity and ionization potential of the Pc aggregates. In addition, four alkyl chains should help increase the solubility of the Pc molecule.

The present chapter focuses on facile preparations of M(TBP) and two new $Cu^{II}Pc$ derivatives. They are synthesized in only two or three steps from the corresponding alkylbenzenes as starting materials. Their abbreviations are shown in Figure 5-1.

§5-2. Synthetic Schemes

The synthetic schemes of the lightly substituted Pc's investigated in this study are shown in Figure 5-2. The previously reported preparation method for derivatives is shown in Figure 5-3. With the methods presented here, Cu(TBP) can be obtained in only two steps. Other related M(TBP) compounds (M=Ni, Pb) and metal-free lightly substituted Pc's prepared in this study and their abbreviations are shown in Figure 5-1.

Metal-free tetra(*tert*-butyl)phthalocyanine (H_2(TBP)) can be obtained in three steps from *tert*-butylbenzene. As an application of this method, two new $Cu^{II}Pc$ derivatives with both alkyl and cyano substituents can be obtained in two steps from the corresponding

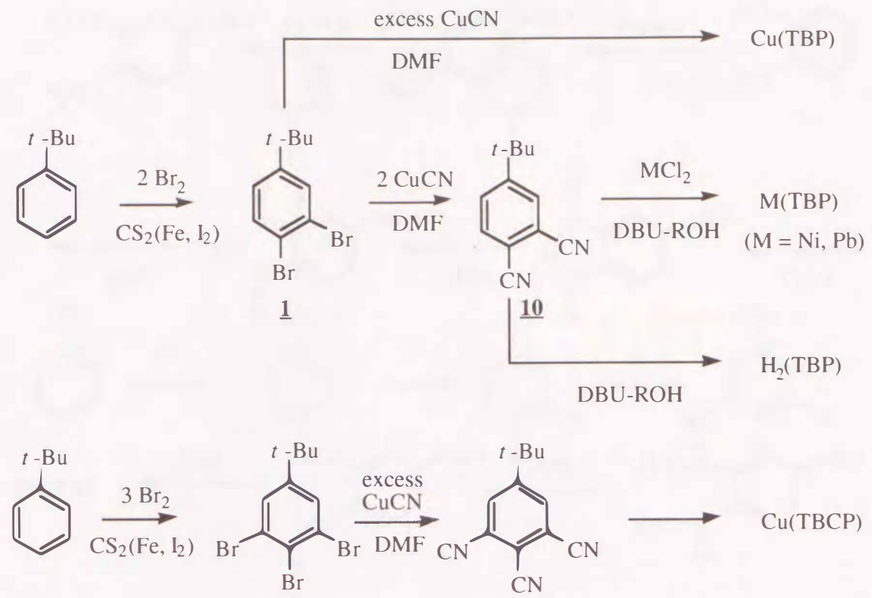

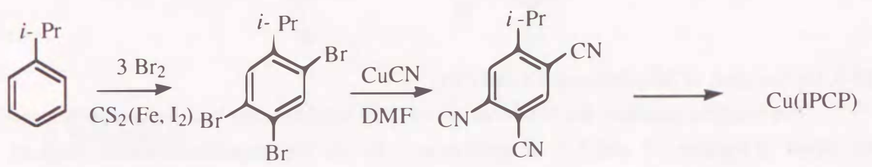

Figure 5-2. Reaction scheme for the lightly substituted phthalocyanine compounds.

alkylbenzenes. These short-cut syntheses basically consist of the following three steps: di- or tri-bromination of alkylbenzene, dicyano or tricyano substitution, and formation of a Pc ring structure.

The bulky *tert-b*utyl moiety acts as a useful positional protective group.[15,16] For example, in the Friedel-Crafts acylation of *tert*-butylbenzene, the acyl group is introduced only at the *para*-position of the benzene.[15] To examine the bromination mechanism, the reaction products were characterized by ^1H and ^{13}C NMR spectroscopies (See Experimental Section).

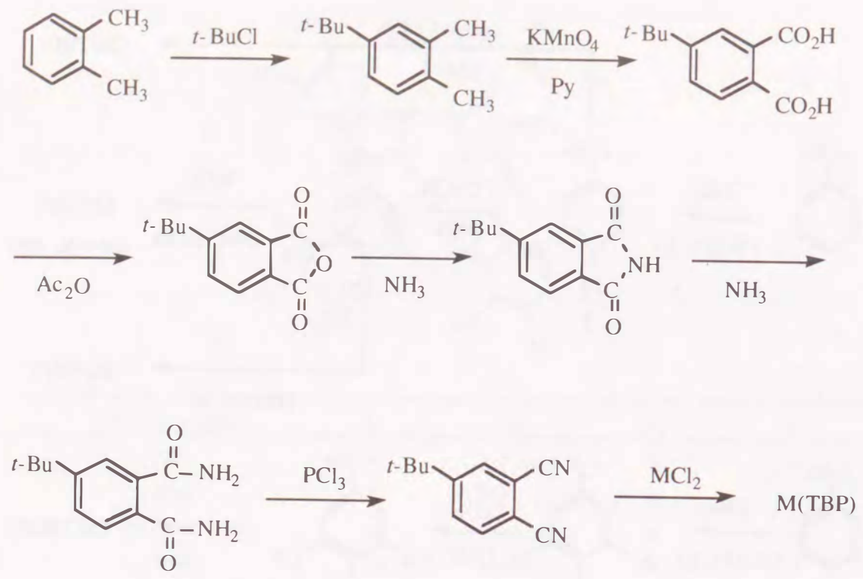

Figure 5-3. Previous preparation method for tetra(*tert*-butyl)phthalocyanine derivatives.

§5-3. Bromination of Alkylbenzene Derivatives

The reaction schemes for bromination of *tert*-butylbenzene and *iso*-propylbenzene are shown in Figures 5-4 and 5-5, respectively. In the first monobromination stage of *tert*-butylbenzene, the product consists of 4-bromo substituted (**2**, major product, 88%) and 3-bromo substituted compounds (**3**, minor product 12%). In the dibromination of *tert*-butylbenzene and further bromination of the mixed monobromo- *tert*-butylbenzenes, a small quantity of *p*-dibromobenzene is isolated.

The monobromination of *tert*-butylbenzene basically occurs only in the *para*-position because of large steric hindrance of the *tert*-butyl moiety. Compound **2**, however, seems to undergo rearrangement or elimination of the *tert*-butyl group, which is catalyzed by proton source in the reaction mixture. In fact, a small quantity of **3** and bromobenzene are produced. Similar rearrangement and elimination of the *tert*-butyl group has already been reported for the acylation of *p-tert*-butyltoluene and polysubstituted *tert*-butylbenzene.[15,16]

When a mixture of **2**, **3** and bromobenzene is further brominated, compound **1** can be obtained from either **2** or **3**, and *p*-dibromobenzene is produced from bromobenzene. When **1** is further brominated, three possible isomers of tribromo- *tert*-butylbenzene (2,3,4-, 3,4,5- (**4**),

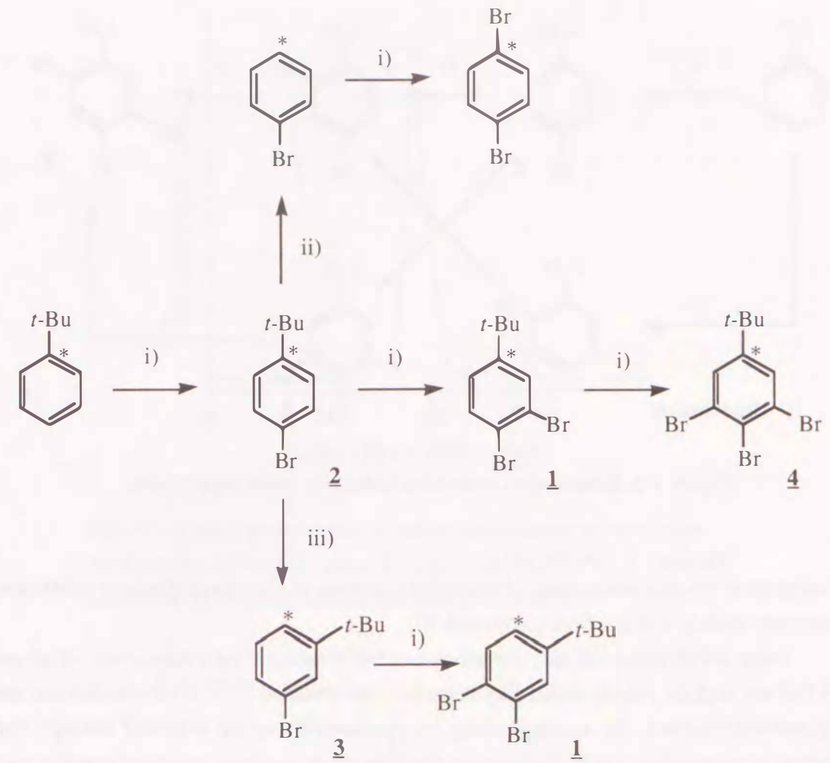

i) Bromination

ii) De-*tert*-butylation

iii) Intramolecular rearrangement of *tert*-butyl group

Figure 5-4. Bromination schemes of *tert*-butylbenzene.
(* indicates the original *ipso*-carbon attached to *tert*-butyl substituents in *tert*-butylbenzene as starting material.)

or 3, 4, 6-positions) are produced. Fortunately, **4** can be easily isolated by recrystallization because of its high molecular symmetry (C_{2v}).

In the bromination of *iso*-propylbenzene, the steric effect of the *iso*-propyl group is much weaker than that of the *tert*-butyl moiety. Monobromo-*iso*-propylbenzenes consist of 4-bromo (**5**, major product, 91%) and 2-bromo substituted compounds (**6**, minor product, 9%). Further bromination of 5 and 6 produced a mixture of 2,4-dibromo (**7**) and 3,4-dibromo

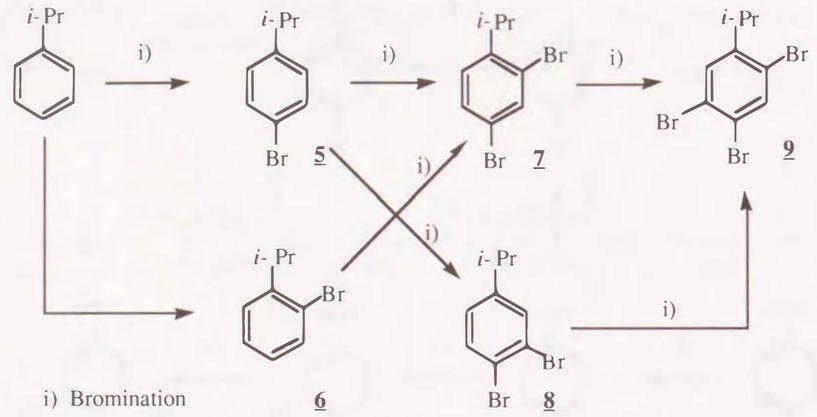

Figure 5-5. Bromination reaction schemes for *iso*-propylbenzene.

(**8**) substituted *iso*-propylbenzenes. Further bromination of the mixed dibromo substituted compounds leads to a single final compound, **9**.

These polybrominated alkylbenzenes can be substituted by cyano anion catalyzed with Cu^{I} ion, and the polycyanated alkylbenzenes are produced.[17,18] From the dicyano and tricyanoalkylbenzenes, the corresponding Pc compounds can be obtained through four consecutive nucleophilic cyclizations by an alkoxide anion in a base-catalyzed reaction such as with diazabicycloundecene (DBU)/*n*-alkanol or CH_3OLi/*n*-alkanol systems.[17-21]

§5-4. Characterization of Geometric Isomers of the Tetra Substituted Phthalocyanines

High performance liquid chromatogram (HPLC) of H_2(TBP) under a reversed mode condition is shown in Figure 5-6. Three signals due to geometric isomers of TBP ring can be resolved. Other M(TBP) analogues (M = Cu, Ni), also, revealed three signals due to their geometric isomers under similar condition. Several attempts to detect geometric isomers of Cu(TBCP) and Cu(IPCP) are failed using HPLC analysis under a normal and reverse mode, due to extremely low solubility in a reverse mode and low resolution in a normal mode.

A ^{1}H NMR spectrum of H_2(TBP) in the -1.5 to -2.5 ppm range is shown in Figure 5-7. Since an integration of three singlets (I, II, III) corresponds to two protons, they are assigned to two internal cavity protons of H_2(TBP). The existence of three peaks proves that H_2(TBP) ring consists of three types among four possible geometric isomers, as shown in Figure 8. Although other M(TBP) analogues (M = Cu, Ni, Pb) and Cu(IPCP) have no such internal cavity protons, several methyl protons due to *tert*-butyl or *iso*-propyl groups can be observed.

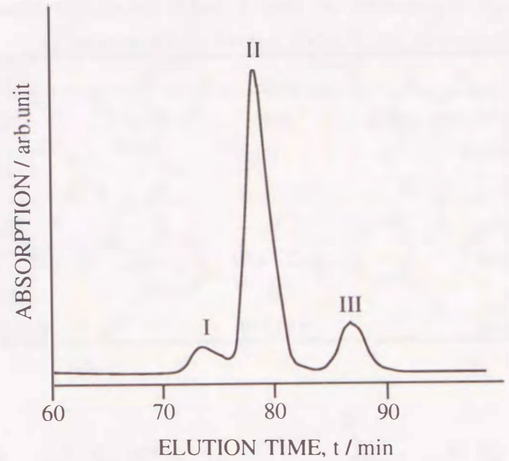

Figure 5-6. High performance liquid chromatograms of metal-free tetra(*tert*-butyl)phthalocyanine (GL-Science Co., ODS-2, 4.7mm ID, EtOH/$CHCl_3$ = 90/10, 30°C, 1 mL/min, l = 670 nm).

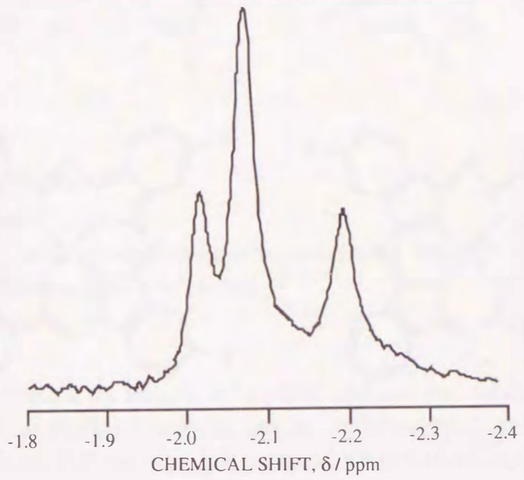

Figure 5-7. Upfield region of ^{1}H NMR spectrum of metal-free tetra(*tert*-butyl)phthalocyanine in C_6D_6.

Table 5-1. Tentative Assignment of Four Possible Geometric Isomers in metal-free tetra(*tert*-butyl)phthalocyanine by ^{1}H NMR and HPLC Measurements.

	C_{4h}	D_{2h}	C_{2v}	C_s
steric hindrance between *tert*-butyl groups	none	large	small	small
the number of reaction type B in TBP ring cyclization[a]	0	2	2	1
^{1}H NMR peak assignment	II		III	I
(observed rel intensity/ppm)	0.52 / -1.72	none	0.16 / -1.78	0.32 / -1.65
HPLC peak assignment	II		III	I
(observed rel peak area/min)	0.73 / 79		0.09 / 73	0.18 / 88

[a] See Figure 5-11.

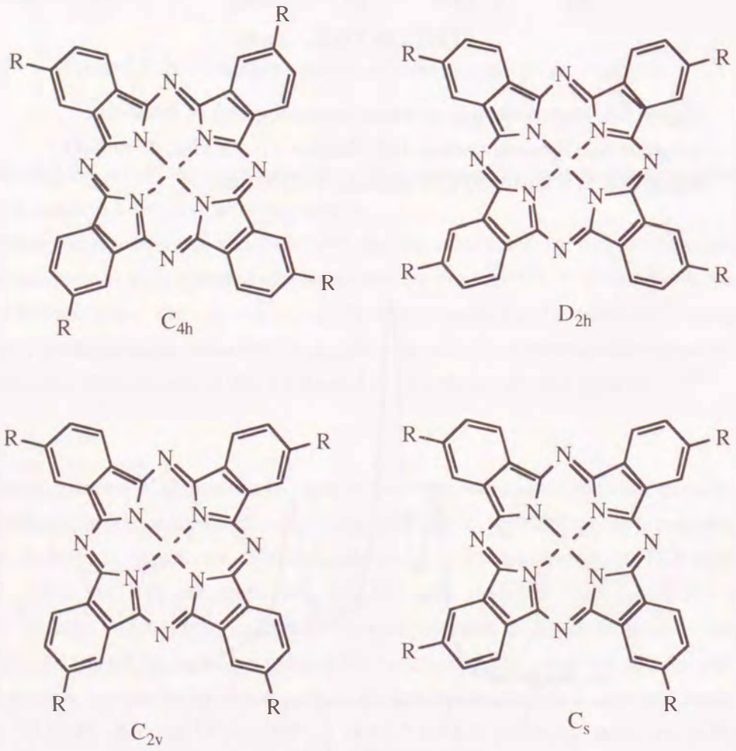

R = *tert*-butyl

Figure 5-8. Four possible geometric isomers of tetra(*tert*-butyl)phthalocyanine ring structures.

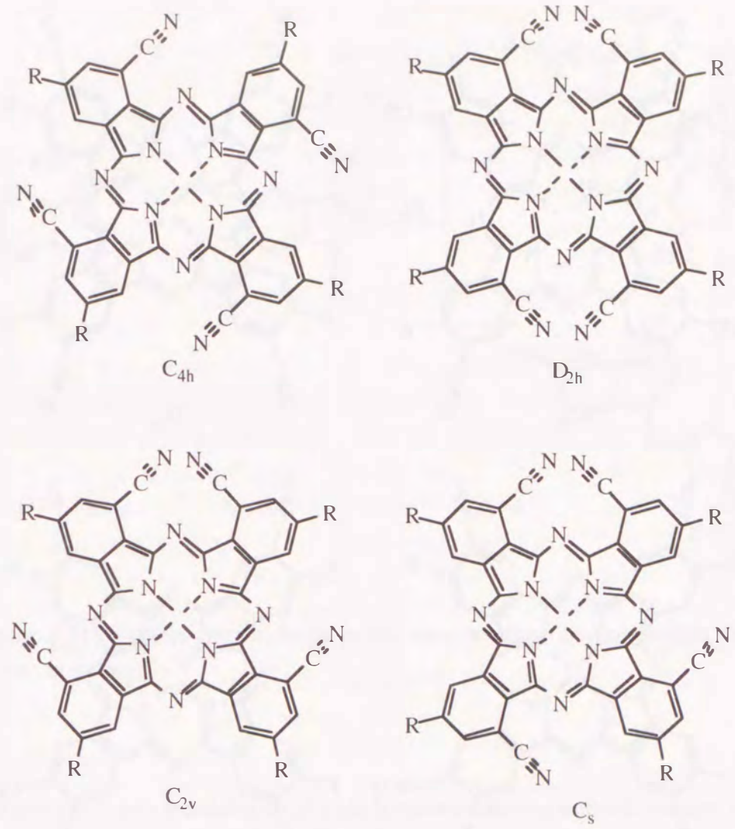

R = *tert*-butyl

Figure 5-9. Four possible geometric isomers of Copper[II] tetra(*tert*-butyl) tetracyanophthalocyanine (Cu(TBCP)).

An assignment of the singlets in ^{1}H NMR spectrum was conducted by considering steric hindrance of *tert*-butyl moieties and the electronic effect of **10** in the TBP ring formation mechanism.[19,20] As illustrated in Figures 5-8 to 5-10, no steric hindrance between *tert*-butyl moieties is presented for the C_{4h} molecule due to its high molecular symmetry. In contrast, the C_{2v} and C_s molecules possess fairly large steric hindrance. The steric hindranceand in the D_{2h} molecule is particularly large.

Figure 5-11 shows the TBP ring formation scheme. There are two cyano sites in **10** for nucleophylic attack of the alkoxide anion in the first stage. From the weak electron

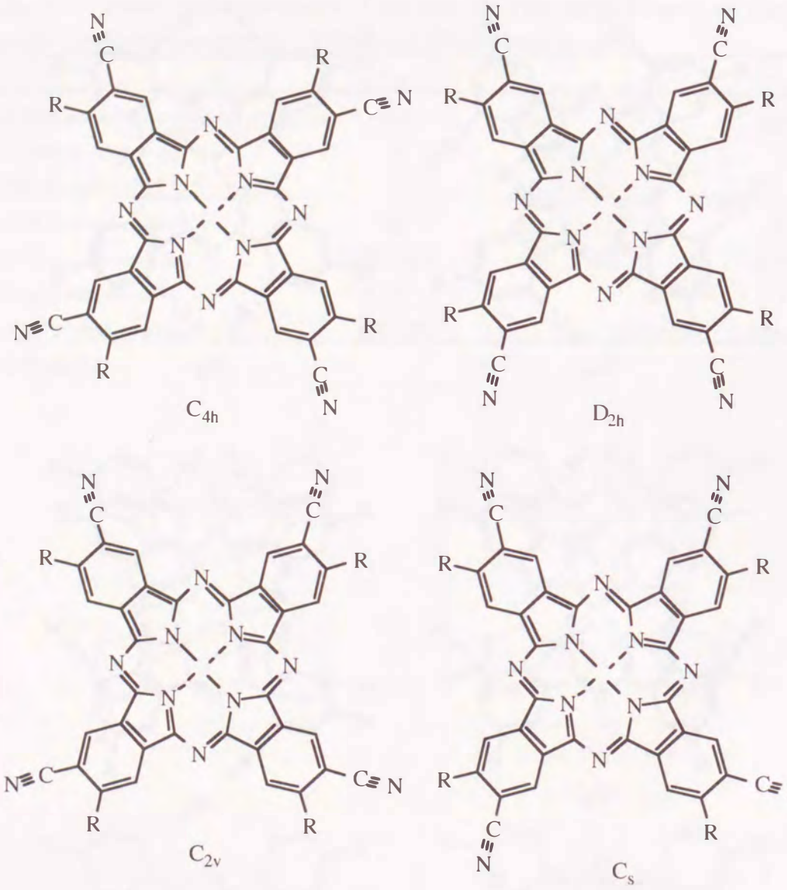

R = *iso*-propyl

Figure 5-10. Four possible geometric isomers of Copper^{II} tetra(*iso*-propyl) tetracyanophthalocyanine (Cu(IPCP)).

donating nature of the*tert*-butyl group, 3-cyano carbon positions are attacked by the anion inpreference to the 4-cyano carbon. In the consecutive cyclization step of **10**, two dimeric intermediates having different configurations (paths A and B) are possible. Paths A and B have 4,4'- and 4,5'-di(*tert*-butyl) configurations, respectively. Although path A is a stereoregular structure, path B leads to irregular structure. Such the number of path B for final TBP products are counted as 0, 2, 2 and 1 for the C_{4h}, D_{2h}, C_{2v}, and C_s molecules.

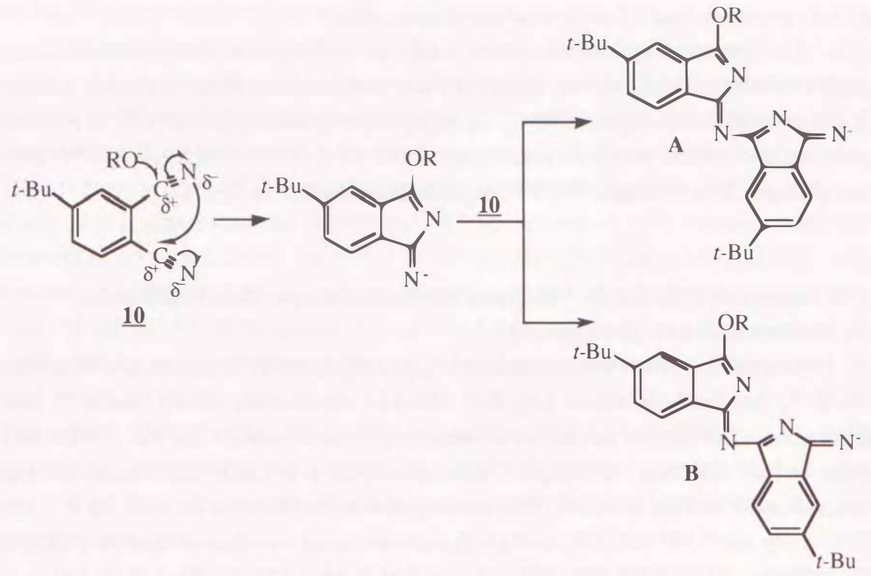

Figure 5-11. Possible intermediates in the tetra(*tert*-butyl)phthalocyanine ring formation scheme.

From the number of path B and degree of steric hindrance mentioned above, the four singlets could be tentatively assigned, as given in Table 5-1.

Cu(TBCP) may contain a single C_{4h} isomer, if stereoregular cyclization of a 3,4,5-tricyano-*tert*-butylbenzene intermediate mainly occurs. From CPK model considerations, **B** type of intermediate cannot hold a planar structure due to large steric hindrance of adjacent two cyano groups, whereas **A** type of intermediate assumes a planar structure. Similarly, CPK models of D_{2h}, C_{2v}, and C_s isomers cannot take planar Pc ring structures and are makedly distorted except for C_{4h} isomer, as expected in Figure 5-9. The idea may be related to the difference in the Q-band characteristics between Cu(TBCP) and Cu(IPCP). Namely, from a comparison of Q-band spectra between Cu(TBCP) and Cu(IPCP) in $CHCl_3$ solution, the absorption maximum of Cu(TBCP) is more strongly blue-shifted than that of Cu(IPCP) by 8 nm, and the absorption intensity of Cu(TBCP) is less than that of Cu(IPCP), despite that both Cu(TBCP) and Cu(IPCP) contain similar electron donating alkyl groups and electron withdrawing cyano groups. Unfortunately, the isomers of Cu(TBCP) and Cu(IPCP) could not be separately assigned even in dilute solutions by NMR spectroscopies due to paramagnetic Cu^{II} ions and by HPLC method using normal or reverse mode.

§5-5. Syntheses of Lead[II] Tetra(*tert*-butyl)phthalocyanine

No synthetic reports have been made on Pb[II] tetra(*tert*-butyl)phthalocyanine (Pb(TBP)) so far. A trace amount of Pb(TBP) was obtained when **10** and PbO were refluxed in 1-chloronaphthalene (bp ca. 270 °C) according to the procedure for PcPb.[18] In a milder condition with DBU/*n*-pentanol system (bp. ca. 130 °C), a relatively high yield of Pb(TBP) was obtained. This is because Pb(TBP) begins to decompose at ca. 200 °C.

§5-6. Preparation of the Lightly Substituted Phthalocyanines and Their Intermediates

(a) 3,4-Dibromo-*tert*-butylbenzene; (**1**).

To a mixture of *tert*-butylbenzene (134 g, 1 mol), I_2 (4.0 g, 16 mmol), and Fe powder (4.0 g, 71 mmol) in 350 mL of CS_2, Br_2 (120 mL, 2.3 mol) was slowly added at room temperature. The mixture was stirred at room temperature overnight and was washed with water and dil $NaHSO_3$. The organic layer was dried over $CaCl_2$ and the solvent was removed under reduced pressure. The resulting oil was distilled in a vacuum. bp 99 - 102 °C/3 mmHg (*lit.*[16] 107-108 °C/3 mmHg). A colorless liquid was obtained and the yield was 222 g (76 %). ^{1}H FT NMR (200 MHz, $CDCl_3$) 7.64 (s, 1H), 7.52 (d, 1H), 7.19 (d, 1H), 1.28 (s, 9H). ^{13}C FT NMR (50 MHz, $CDCl_3$, relative intensity) 151.9 (0.58), 133.2 (0.23), 131.1 (0.23), 126.2 (0.32), 124.6 (0.51), 120.8 (0.48), 34.9 (0.99), 31.0 (1.00). A first fraction (bp 82 °C/3 mmHg) was identified as *p*-dibromobenzene and the yield was 5.5 g. Anal. Found: C,30.32; H,1.84. Calcd for $C_6H_4Br_2$ (the first fraction): C, 30.55; H, 1.71. ^{1}H FT NMR 7.55 (s, 4H). The third fraction (bp 127-128 °C/3 mmHg) was a mixture of tribromo-*tert*-butylbenzene isomers, as described later, and the yield was 19 g.

(b) 4-Bromo-*tert*-butylbenzene (**2**).

To clarify the dibromination mechanism of *tert*-butylbenzene, the reaction product of monobromo-*tert*-butylbenzene was examined. To a mixture of *tert*-butylbenzene (27.4 g, 0.20 mol), Fe powder (0.1 g), I_2 (0.1 g) in 50 mL of CS_2, Br_2 (11.5 mL, 0.22 mol) was slowly added at 2-5 °C and reacted at that temperature for 15 min. After the reaction mixture was treated in the same manner as in the preparation of **1**, crude product **2** was obtained under reduced pressure. bp 71 - 72 °C/3 mmHg. A colorless liquid was obtained and the yield was 24.3 g (57 %). ^{1}H FT NMR ($CDCl_3$) 7.401 (d, 2H), 7.247 (d, 2H), 1.29 (s, 9H) and 7.45 - 7.20 (m), 1.31 (s). ^{13}C FT NMR ($CDCl_3$) 149.8 (0.13), 130.9 (0.92), 127.0 (1.0), 119.1 (0.19), 34.2 (0.10, $(CH_3)_3C$-), 31.1 (1.0, $(CH_3)_3C$-) and 157.7 (0.022), 150.7 (0.011), 127.9 (0.12), 125.2 (0.072), 125.0 (0.11), 34.4 (0.011, $(CH_3)_3C$-), 31.2 (0.14, $(CH_3)_3$ C-). ^{13}C FT NMR spectra showed that the product consists of **2** (88%) and *m*-bromo-*tert*-butylbenzene (**3**, 12%).

(c) 3,4,5-Tribromo-*tert*-butylbenzene (**4**).

To a mixture of *tert*-butylbenzene (54 g, 0.4 mol), Fe powder (0.5 g), and I_2 (0.5 g) in 100 mL of CS_2, Br_2 (21 mL, 0.4 mol) was slowly added at 2-5 °C. Additional Br_2 (42 ml, 0.8 mol) was then added at room temperature. After stirring at room temperature overnight, the reaction mixture was treated in the usual way and was distilled under reduced pressure. The first fraction (bp 70 °C/3 mmHg) crystallized and the yield was 6.7 g (7.1 %). This was identified as *p*-dibromobenzene from IR and ^{1}H NMR spectra. A crude colorless liquid was obtained as the main fraction. bp 127 - 134 °C/3 mmHg, Crude yield, 122 g (82 %). This fraction was determined to be a mixture of several isomers of tribromo-*tert*-butylbenzene from ^{1}H and ^{13}C FT NMR spectra. Compound **4** was isolated by recrystallization of the crude tribromo-*tert*-butylbenzenes from EtOH. Colorless needles were obtained and the yield was 30.2 g (20 %). Anal. Found: C, 32.49; H, 3.12. Calcd for $C_{10}H_{11}Br_3$: C, 32.38; H, 2.99. ^{1}H FT NMR ($CDCl_3$) 7.56 (s, 2H), 1.29 (s,9H). ^{13}C FT NMR ($CDCl_3$) 153.7 (0.09), 130.5 (0.64), 126.2 (0.22), 124.4 (0.09), 35.3 (0.10), 31.4 (1.00). Compound **4** was also prepared by further bromination of 3,4-dibromo-*tert*-butylbenzene according to the same procedure as **2**.

(d) 4-Bromo-*iso*-propylbenzene (**5**).

This was prepared by the same procedure as **2** using *iso*-propylbenzene instead of *tert*-butylbenzene as starting material. bp 59-60 °C/3 mmHg. A colorless liquid was obtained and the yield was 80.0 g (67 %). ^{1}H FT NMR ($CDCl_3$) 7.39 (d, 2H), 7.07 (d, 2H), 2.84 (sept, 1H), 1.20 (d, 6H) and 7.5-6.9 (m), 3.35 (sept), 1.25 (d). ^{13}C FT NMR ($CDCl_3$) 148.3 (0.37), 131.8 (0.98), 128.7 (1.0), 34.2 (0.63), 24.4 (0.97) and 148.0 (0.05), 133.5 (0.05), 128.0 (0.05), 127.6 (0.05), 127.2 (0.07), 118.2 (0.05), 33.5 (0.03), 23.2 (0.10). From ^{1}H and ^{13}C FT NMR spectra, the product was identified as a mixture of **5** (91 %) and 2-bromo-*iso*-propylbenzene (**6**, 9%).

(e) Dibromo-*iso*-propylbenzenes (**7** and **8**).

These were prepared by further bromination of a mixture of **5** and **6** and by direct dibromination of *iso*-propylbenzene. bp 90 - 92 °C/4 mmHg. A colorless liquid prepared by dibromination of *iso*-propylbenzene was obtained and the yield was 17.1 g (61 %). ^{1}H FT NMR ($CDCl_3$) 7.7-6.9 (m, 2H), 3.30 (sept, 0.64H), 2.83 (sept, 0.36H), 1.20 (d, 6H). ^{13}C FT NMR ($CDCl_3$) 149.8 (0.20), 135.0 (0.46), 130.8 (0.50), 127.9 (0.50), 124.8 (0.29), 119.7 (0.25), 32.5 (0.56), 22.7 (1.00) and 146.4 (0.31), 133.5 (0.31), 131.8 (0.32), 126.9 (0.38), 124.7 (0.17), 33.5 (0.31), 23.7 (0.64). From ^{1}H and ^{13}C FT NMR spectra, the product was identified as a mixture of 2,4-dibromo-*iso*-propylbenzene (**7**, 64-70 %) and 3,4-dibromo-*iso*-propylbenzene (**8**, 36-30 %).

(f) 2,4,5-Tribromo-*iso*-propylbenzene (**9**).

This was prepared by further bromination of a mixture of **7** and **8** and by direct tribromination of *iso*-propylbenzene. bp 108-111 °C/4 mmHg. A colorless liquid by tribromination of *iso*-propylbenzene was obtained and the yield was 36.2 g (50 %). ^{1}H FT NMR 7.77 (s, 1H), 7.47 (s, 1H), 3.25 (sept,1H), 1.20 (d, 6H). ^{13}C FT NMR 148.4 (0.39), 136.7 (0.54), 131.5 (0.54), 124.0 (0.29), 123.2 (0.31), 122.4 (0.28), 32.7 (0.65), 22.6 (1.00).

(g) 3,4-Dicyano-*tert*-butylbenzene (**10**).

A mixture of **1** (44 g, 0.15 mol) and CuCN (40 g, 0.44 mol) was gently refluxed in dimethylformamide (DMF, 300 mL) for several hours. A mixture of conc NH_3 (100 mL) and water (300 mL) was added to the reaction mixture, and O_2 gas was fully bublled into the mixture. The reaction mixture was filtered under reduced pressure and the resulting solid was dissolved in $CHCl_3$. After being dried over Na_2SO_4 overnight, the solvent was removed under a reduced pressure. The residual dark green oil was recrystallized from methylcyclohexane. A green solid was obtained with a crude yield of 21.3 g (76 %). The crude product was purified by sublimation *in vacuo*. A white solid was isolated with a yield of 11.7 g (42 %). Anal. Found: C, 78.48; H, 6.75, N,15.20. Calcd for $C_{12}H_{12}N_2$: C, 78.23; H, 6.57; N, 15.20. ^{1}H FT NMR ($CDCl_3$) 7.80 (s, 1H), 7.75 (s, 2H), 1.38 (s, 9H). ^{13}C FT NMR ($CDCl_3$) 158.0 (0.14), 133.7 (0.28), 131.2 (0.29), 130.9 (0.28), 116.2 (0.14), 115.9 (0.16), 115.8 (0.18, 4-CN), 112.9 (0.19, 3-CN), 35.9 (0.25), 30.9 (1.0).

(h) Copper^{II} Tetra(*tert*-butyl)phthalocyanine (Cu(TBP)).

A mixture of **1** (5.82 g, 20 mmol) and CuCN (5.4 g, 60 mmol) was allowed to react in DMF (25 mL) at 165 °C for a day. After dil NH_3 was added to the reaction mixture, the crude product was extracted with $CHCl_3$. After removing the solvent, 2.87 g of the crude product were obtained. The product was purified using column chromatography (silica gel, chloroform). A blue powder was isolated and the yield was 1.85 g (46 %). Anal. Found: C, 71.69; H, 6.13; N, 14.15. Calcd for $C_{48}H_{48}N_8Cu$: C, 72.02, H, 6.04, N, 14.00. vis(λ_{max}(ε), $CHCl_3$) 677nm ($2.6{\cdot}10^5$ $M^{-1}{\cdot}cm^{-1}$).

(i) Nickel^{II} Tetra(*tert*-butyl)phthalocyanine (Ni(TBP)).

A mixture of **1** (0.92 g, 5.0 mmol), $NiCl_2$ (0.20 g, 1.54 mmol), and diazabicycloundecene (DBU, 1.54 g, 10.1 mmol) was gently refluxed in *n*-butanol (20 mL) for 5 h. The product was purified in the same procedure as Cu(TBP). A blue solid was obtained and the yield was 0.30 g (30 %). Anal. Found: C, 72.26; H, 5.99; N, 13.94. Calcd for $C_{48}H_{48}N_8Ni$: C, 72.46; H, 6.08; N, 14.08. ^{1}H FT-NMR 8.9 (m, 4H), 8.6 (m, 4H), 8.0 (m, 4H), 1.85 (m, 36H). vis (λ_{max}(ε), $CHCl_3$) 670 nm ($1.9{\cdot}10^5$ $M^{-1}{\cdot}cm^{-1}$).

(j) Lead^{II} Tetra(*tert*-butyl)phthalocyanine (Pb(TBP)).

A mixture of **1** (0.92 g, 5 mmol), $PbCl_2$ (0.42 g, 1.51 mmol), and DBU (1.5 g, 10 mmol) was gently refluxed in *n*-pentanol (15 mL) for a day. The product was isolated as green prism in a manner similar to Cu(TBP). The yield was 0.19 g (16 %). Anal. Found: C, 59.72; H, 5.41; N, 11.16. Calcd for $C_{48}H_{48}N_8Pb$: C, 61.06; H, 5.12; N, 11.87. ^{1}H FT NMR ($CDCl_3$) 9.0 (m, 4H), 8.8 (m, 4H), 8.2 (m, 4H), 1.7 (d, 36H). vis(λ_{max}(ε), $CHCl_3$) 721 nm ($1.2{\cdot}10^5$ $M^{-1}{\cdot}cm^{-1}$).

(k) Metal-free Tetra(*tert*-butyl)phthalocyanine (H_2(TBP)).

A mixture of **1** (0.46 g, 2.5 mmol) and CH_3OLi (0.3 g, 7.5 mmol) was gently refluxed in *n*-pentanol (5 mL) for a day. The product was isolated in a manner similar to Cu(TBP). A red purple solid was obtained and the yield was 0.20 g (54 %). Anal. Found: C, 77.58; H, 6.77; N, 14.87. Calcd for $C_{48}H_{50}N_8$: C, 78.02; H, 6.82; N, 15.16. ^{1}H FT NMR ($CDCl_3$) 9.4-9.0 (m, 8H), 8.2 (t, 4H), 1.8 (m, 36 H), -2.1 (three singlets, 2H). vis(λ_{max}(ε), $CHCl_3$) 699 nm ($1.38{\cdot}10^5$ $M^{-1}{\cdot}cm^{-1}$), 663 nm ($1.19{\cdot}10^5$ $M^{-1}{\cdot}cm^{-1}$).

(l) Copper^{II} Tetra(*tert*-butyl)-tetracyanophthalocyanine (Cu (TBCP)).

A mixture of **4** (3.6 g, 10 mmol) and CuCN (5.4 g, 60 mmol) in DMF (50 mL) was gently refluxed for a day. The product was purified by the same manner as Cu(TBP). A blue solid was isolated and the yield was 0.43 g (19 %). Anal. Found: C, 68.57; H, 5.02; N, 18.44. Calcd for $C_{52}H_{44}N_{12}Cu$: C, 69.35; H, 4.92; N, 18.66. ^{1}H FT NMR ($CDCl_3$) 1.8 (br, s). vis(λ_{max}(ε), $CHCl_3$) 676 nm ($1.23{\cdot}10^5$ $M^{-1}{\cdot}cm^{-1}$).

(m) Copper^{II} Tetra(*iso*-propyl)-tetracyanophthalocyanine (Cu(IPCP)).

A mixture of **9** (14.9 g, 43 mmol) and CuCN (18 g, 0.3 mol) was refluxed in DMF (100 mL) for a day. The product was purified by the same procedure as Cu(TBP). A red purple solid was obtained and the yield was 1.7 g (29.8 %). Anal. Found: C, 67.93; H, 4.56; N, 19.54. Calcd for $C_{48}H_{36}N_{12}Cu$: C, 68.27; H, 4.30; N, 19.90. ^{1}H FT NMR ($CDCl_3$) 4.5 (br, s, 4H), 1.55 (br, s, 24H). vis(λ_{max}(ε), $CHCl_3$) 684 nm ($1.80{\cdot}10^5$ $M^{-1}{\cdot}cm^{-1}$).

§5-7. Conclusion

Several related metallo and metal-free Pc compounds having short alkyl chains (*tert*-butyl or *iso*-propyl) and/or cyano groups were prepared. Soluble phthalocyanines with cyano substituents were newly obtained. These Pc's were synthesized from alkylbenzene in only two or three steps with excellent yields. The previously reported method for tetra(*tert*-butyl)phthalocyanine ring required seven steps from *o*-xylene. These substituted Pc's consist of three of four possible geometric isomers, since metal-free tetra(*tert*-butyl)phthalocyanine has three singlets of internal cavity protons. Although only Cu^{II} tetra(*tert*-butyl)-

tetracyanophthalocyanine has a possibility to be a single type of isomer with C_{4h} molecular symmetry from its Q-band spectrum and reaction mechanism of intermediates with steric hindrance, NMR and HPLC analyses cannot confirm this possibility. Lead^{II} tetra(*tert*-butyl)-phthalocyanine was prepared for the first time but was unstable in heat, water, or air.

§5-8. References

1. Loutfy, R. O.; Sharp, J. H. *J. Chem. Phys.* **1979**, *71*, 1211.
2. Tang, C. W. *Appl. Phys. Lett.* **1986**, *48*, 183.
3. Arishima, K.; Hiratsuka, H.; Tate, A.; Okada, T. *Appl. Phys. Lett.* **1982**, *40*, 279.
4. Kato, M.; Nishioka, Y.; Kaifu, K.; Kawamura,K.; Ohno,S. *Appl. Phys. Lett.* **1985**, *46*, 196.
5. Loutfy, R. O.; Hor, A. M.; DiPaola-Baranyi, G.; Hsiao, C. K. *J. Imag. Sci.* **1985**, *29*, 116.
6. Honeybourne, C. L.; Ewen, R. J.; Hill, C. A. S. *J. Chem. Soc. Faraday Trans. 1.* **1984**, *80*, 851.
7. Moskalev, P. N.; Kirin, I. S. *Rus. J. Phys. Chem.* **1972**, *46*, 1019.
8. Yamamoto, H.; Sugiyama, T.; Tanaka, M. *Jpn. J. Appl. Phys.* **1985**, *24*, L305.
9. Hann, R. A.; Gupta, S. K.; Fryer, J. R.; Eyres, B. L. *Thin Solid Films* **1985**, *134*, 35.
10. Kovacs, G. J.; Petty, M. C.; Baker, S.; Fowler, M. T.; Thomas, N. J. *Thin Solid Films* **1985**, *133*, 197.
11. Roberts, G. G.; Petty, M. C.; Baker, S.; Fowler, M. T.; Thomas, N. J. *Thin Solid Films* **1985**, *132*, 113.
12. Mikhalenko, S. A.; Barkanova, S. V.; Lebedev, O. L.; Luk'yanets, E. A. *Zh. Obshch. Khim.* **1971**, *41*, 2735.
13. Larner B. W.; Peters, A. T. *J. Chem. Soc.* **1952**, 680.
14. Contractor, R. B.; Peters, A. T. *J. Chem. Soc.* **1949**, 1314.
15. Heintzelman, W. J.; Corson, B. B. *J. Org. Chem.* **1957**, *22*, 25.
16. Tashiro, M.; Yamato, T. *J. Chem. Soc. Perkin I* **1978**, 176.
17. Pawlowski, G.; Hanack, M. *Synthesis* **1980**, 287.
18. Fujiki, M.; Tabei, H. *Langmuir* **1988**, *4*, 320.
19. Tomoda, H.; Saito, S.; Ogawa, S.; Shiraishi,S. *Chem. Lett.* **1980**, 1277.
20. Oliver, W. Stuart; Smith, Thomas D. *J. Chem. Soc. Perkin Trans. Part 2* **1987**, 1579.
21. Kroenke, W. J.; Kenney, M. E. *Inorg. Chem.* **1964**, *3*, 251.

CHAPTER 6

CHARACTERIZATION OF LANGMUIR-BLODGETT FILMS OF PHTHALOCYANINES WITH SHORT ALKYL SUBSTITUENTS

SYNOPSIS

The molecular arrangement and orientation in Langmuir-Blodgett films of several phthalocyanines (Pc's) containing *tert*-butyl, *iso*-propyl, and cyano groups are examined. These films are prepared by the horizontal lifting technique. The force-area data, Q-band spectra of the films, and *d*-spacing in powder X-ray diffraction patterns suggest that these Pc's take one-dimensionally assembled structures and edge-on configurations relative to the air-water interface. Also, the dependence of the Q-band absorption intensity on the incident light angle in polarized visible spectroscopy was consistent with the above Pc configuration.

§6-1. Introduction

Based on the use of potential applications for photonic and electronic devices, thin films of phthalocyanines (Pc's) have been of particular interest for many years.[1-9] Thin films of unsubstituted Pc's usually were made by vacuum evaporation or dispersion in a polymer binder, because they usually exist in various polymorphic forms in the solid state and poor solubility in common organic solvents.

Recently, the Langmuir-Blodgett (LB) technique has been noted as a suitable way of ultrathin films of soluble Pc's. Several workers have studied the preparation, structure and electrical properties of LB films based on Pc's with short substituents such as *tert*-butyl, isopropylaminomethyl, and cumylphenoxy groups.[11-20] Other researchers have characterized the LB films of Pc's involving long alkyl chains such as octadecoxy and octadecylamide.[17,21-23] Our main interest concerns how to control the lattice architecture and electronic delocalization in thin films for microelectronic devices based on organic substances. As a first attempt to obtain a highly conducting substance formed by the LB technique, we have demonstrated thin film of tetrathiafulvalene-tetracyanoquinodimethane with 5.5 $S \cdot cm^{-1}$ without any dopants.[24]

In Chapters 2 to 4, it has demonstrated that two types of NiPc's with four long chain alkyl amide substituents are in one-dimensional self-assembled structures in solids and in solution and can form good quality LB films. The LB film conductivities of these Pc's were, however, not so affected by exposure to an electron acceptor because of existence of insulating long alkyl moieties. In Chapter 5, we designed two new types of Cu^{II} tetracyanophthalocyanines substituted with short alkyl groups in order to imrpove the LB

film formation and doping effect. This chapter discussed the molecular arrangement and orientation of LB films of the new Cu^{II} tetracyanophthalocyanines and three tetra(*tert*-butyl)phthalocyanine derivatives (M(TBP), M is central metal).

§6-2. Force-Area Isotherms

Figure 6-1 displays force-area isotherms of the Pc's with short alkyl substituents and unsubstituted metal-free Pc on pure water at 5 °C. The limiting areas of M(TBP) (M = Ni, Cu, H_2) cover 32 to 43 $Å^2$/molecule which are completely different from previously reported data for Cu(TBP) and H_2(TBP).[11-13] Although TBP derivatives are reported to provide high quality LB films, the force-area isotherms depend strongly on the laboratory techniques.[11-13,17] Careful selection of the experimental conditions, such as spreading solvents, additives in the subphase, subphase temperature and TBP concentration, is required to obtain a reproducible monolayer film at the air-water interface. In contrast, Cu(TBP) and Cu(IPCP) which involve polar cyano moieties invariably form a reproducible and fairly stable monolayer at the air-water interface independently of particular conditions.

Pb(TBP) did not yield reproducible force-area curves, because of decomposition of Pb(TBP) molecule at the air-water interface. Pb(TBP) appears to be less stable under exposure to heat, light, and water. In fact, the color of Pb(TBP) in dilute $CHCl_3$ solution completely changed from green to colorless when it came in contact with water or was placed under a room light overnight.

If Pc molecules take an edge-on configuration at the air-water interface, the resulting limiting areas for Cu(TBCP) and Cu(IPCP) are 69 and 75 $Å^2$/molecule, respectively. They are almost identical to the previously reported calculated areas for lightly substituted Pc molecules (62 $Å^2$/molecule for Cl_2Si(TBP) and 68 $Å^2$/molecule for tetra(cumylphenoxy) Pc's).[14,17]

§6-3. UV-Visible Absorption Spectra

Figure 6-2 shows UV-visible absorption spectra of M(TBP) (M = Cu, Ni, H_2, Pb), Cu(TBCP), and Cu(IPCP) in LB films prepared by the horizontal lifting technique and in solution. The Q-band of M(TBP)s (M = Cu, Ni, H_2) in LB films are broad and strongly blue-shifted by 1200 to 1300 cm^{-1}, compared to the corresponding monomeric Q-band spectra in solution. The visible absorption spectra of Cu(TBP) and H_2(TBP) in LB films are almost identical to the previously reported spectra.[11,13] Also, the Q-band of Cu(TBCP) and Cu(IPCP) in LB films are broader and blue-shifted by 1000 to 1100 cm^{-1} more than those of the corresponding monomeric Q-band in solution. In contrast, the Q-band of Pb(TBP) in LB film is close to that of the monomeric state in solution.

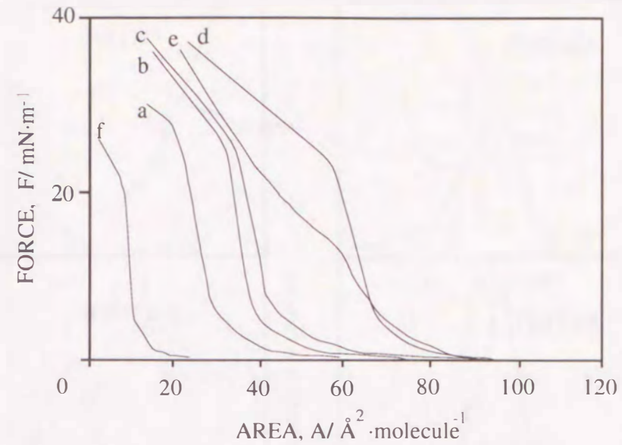

Figure 6-1: Force-area isotherms of the Pc's with short substituents.
(a; Cu(TBP), b; Ni(TBP), c; H_2(TBP), d; Cu(TBCP), e; Cu(IPCP), f; H_2(Pc) from Li_2(Pc)) Unsubstituted H_2(Pc) LB film was prepared by the reported procedure, in which Li_2(Pc) in acetone is spread on the air-water interface then hydrolyzed *in situ*.[11]

Such marked broadening and blue-shifts in the Q-band spectra seem to be characteristic of the Q-band spectra of one-dimensional, linear stacked Pc systems with van der Waals' thickness. For example, the Q-band of O-linked tetra (*tert*-butyl) PcM polymers (M = Si, Ge) are broad and strongly blue-shifted by 1300 to 1640 cm^{-1}, compared to the corresponding monomeric states. In contrast, evaporated films of β-Cu(Pc) and β-H_2(Pc) which exist in obliquely stacked structures show two red-shifted Q-bands compared to the monomer Q-band.[26,27] Previous workers have considered that H_2(TBP) in an LB film that shows a blue-shifted Q-band takes an obliquely stacked structure with a tilt angle of 52°.[13] However, according to the molecular exciton theory, the angle should correspond to a small red-shifted Q-band.[28] Recently, another group has revealed from an ESR study that Cu(TBP) molecules doped in an H_2(TBP) LB film are vertically aligned on the substrate plane.[16]

§6-4. Powder X-Ray Diffraction Patterns

Figure 6-3 shows X-ray diffraction patterns of lightly substituted Pc's in solids. Except for Pb(TBP), the characteristic patterns of the Pc can be invariably seen in a range of $2\theta = 26° - 27°$. This indicates that the Pc's have a *d*-spacing of 3.3 to 3.4 Å, which correlates

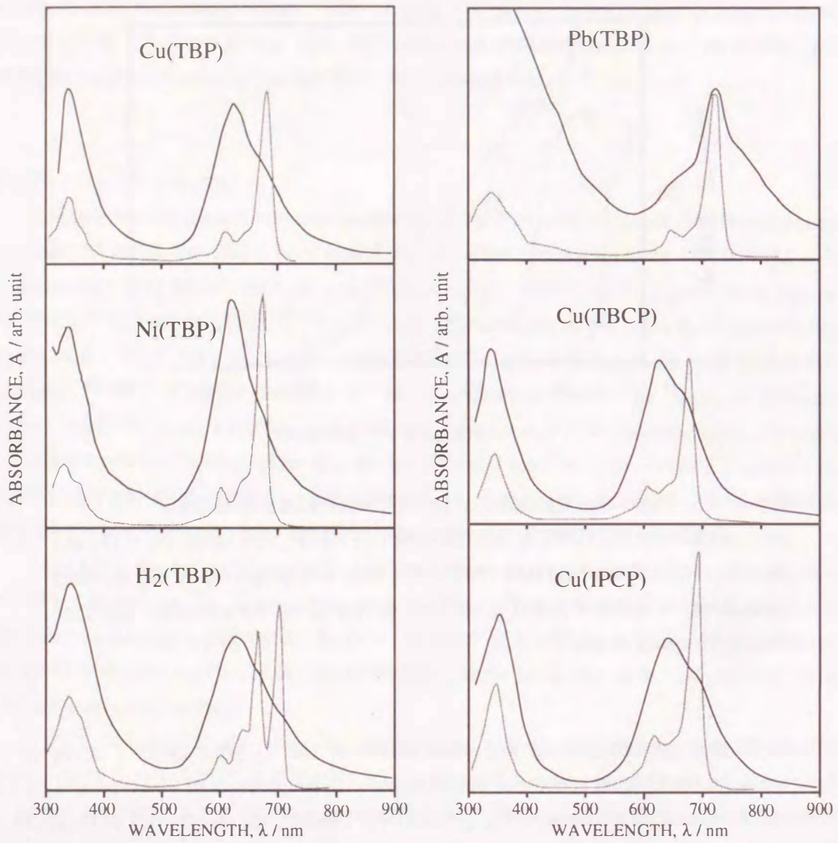

Figure 6-2. Electronic absorption spectra of M(TBP) (M = Cu, Ni, H_2, Pb), Cu(TBCP), and Cu(IPCP) in LB films prepared by the horizontal lifting technique (solid line) and in solution (dotted line).

to the closest ring spacing of the Pc stack. Visible absorption spectra of the Pc's in LB films are identical to those in solids. This means that the ring stack arrangement of these in LB films is basically identical to that in solids, though a number of the stacks in LB films may differ from those in solids.

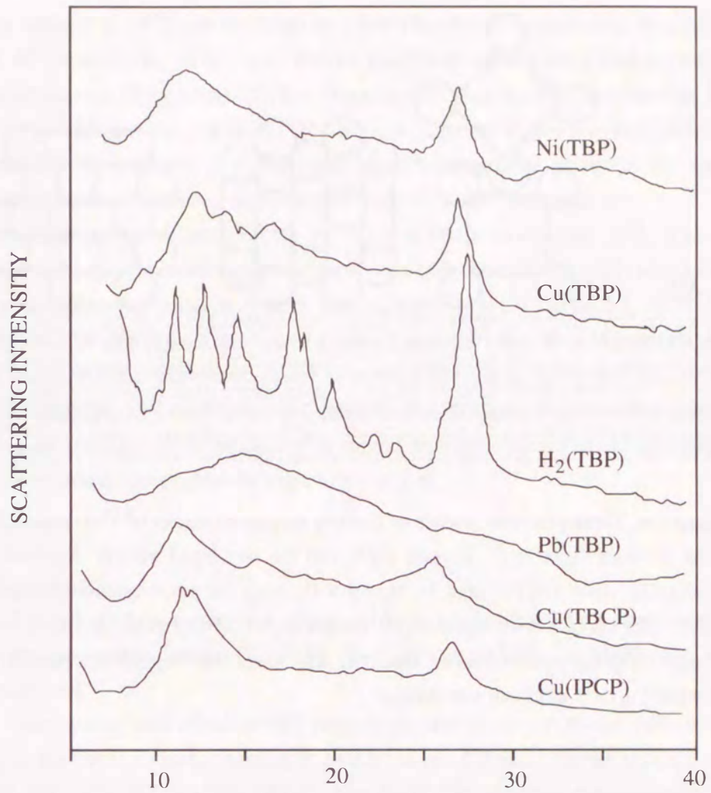

Figure 6-3. X-ray diffraction patterns of lightly substituted Pc powders (Cu K_α).

§6-5. Assembled Structures

Kovacs *et al.*[13] and Barger *et al.*[17] considered three possible orientations of the Pc macrocycle at the air-water interface; (1) Pc rings vertical to the interface. (2) Pc rings tilted against the interface. (3) Pc rings parallel to the interface forming multilayers. For lightly substituted Pc derivatives, they considered two possibilities; linear-staggered and slip-eclipsed stack structures. Kovacs *et al.* claimed from the force-area isotherm, electronic absorption spectra and X-ray diffraction data of the Pc powder that the H_2(TBP) rings are perpendicular to the water surface and are stacked obliquely.[13] Barger *et al.* supposed that tetra(cumylphenoxy)Pc rings are parallel to the surface and take a slipped stack of ten molecules, since in a mixed film of the Co^{II}phthalocyanine derivative and octadecanol the Pc rings are concluded to be parallel to the surface from resonance Raman spectroscopy.[17]

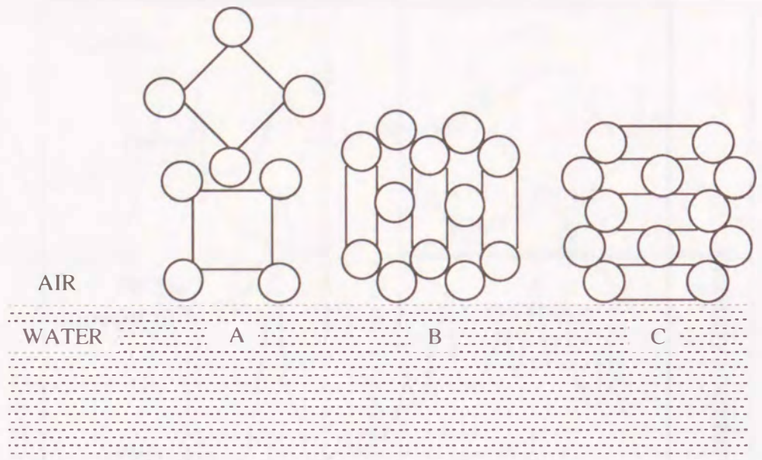

Figure 6-4. Three possible models of linearly staggered stacks of TBP molecules at the air-water interface. (Circles represent the *tert*-butyl moiety. Squares or rectangulars represent Pc rings. In Model A Pc rings are perpendicularly aligned to the water surface with bimolecular thickness, in Model B the stacking axes are parallel to the water surface. Model C represents that Pc rings are parallel to the water surface and form a multilayer.)

To explain the marked blue-shifts of Q-band spectra and the closest ring separation with van der Waals' thickness in the present Pc systems, the lightly substituted Pc's, except for Pb(TBP), are expected to be in linear-staggered stacking structures, not slipped or not eclipsed, with the closest Pc ring separation. If the Pc rings with four bulky *tert*-butyl moieties take a linearly eclipsed structure, the rings cannot approach each other as close as van der Waals' thickness and if the rings are in slipped stacking structures, the blue-shift Q-band would not be observed. Four bulky substituents of TBP ring would help assembling it in a linearly staggered state as expected from its CPK space filling model consideration.

Three possible arrangements of linearly staggered stacks of TBP molecules on the water are shown in Figure 6-4. Circles represent the tert-butyl moiety. Squares or rectangulars represent Pc rings. Models A and B show that Pc rings are perpendicularly aligned to the water surface and the stacking axes are parallel to the water surface. In such a case, the film thickness is estimated to be 20 Å/layer from a CPK space filling model of the Pc's. In model A, Pc molecules form a bilayer. Model C represents Pc rings that are parallel to the water surface and form a multilayer. Assuming that a Pc ring edge is 20 Å thick and

the ring spacing is 3.4 Å, the occupied area per molecule is evaluated as 34 $Å^2$ for model A and 68 $Å^2$ for model B. In model C, the occupied area depends on a stacking number. If Pc molecules are in a 12 molecular stack in model C, the area is 33 $Å^2$, the same as in model A. Also, if Pc molecules are in a six molecular stack in model C, the area is 67 $Å^2$, the same as in model B. Accordingly, it is not clear which arrangement exists on the water from a comparison between the force-area isotherm and calculated molecular area.

Recently, direct observation of the Cu(TBP) monolayer with high-resolution transparent electron microscopy clearly showed that most of the TBP molecules take an edge-on configuration (models A or B) but are partially lying flat to the substrate.[29,30] All Pc arrays in TBP derivatives must form a bilayer with the edge-on configuration, as shown in model A, since the observed occupied area per molecule is about half the corresponding value for model B. In Cu(TBCP) and Cu(IPCP), the Pc stacks will exist in a monolayer with the edge-on configuration, as shown in model B, since the observed occupied area per molecule is almost identical to the value for model B.

§6-6. Conclusion

The LB film characteristics of several lightly substituted Pc's containing *tert*-butyl, *iso*-propyl, and cyano groups (M(TBP), M(TBCP) and M(IPCP), M=Ni, Cu, Pb and H_2) were examined.

The limiting area of the surface monolayer, broadening and blue-shifts in the Q-band spectra of the LB films and *d*-spacing in powder X-ray diffraction patterns of the suggest that M(TBP) (M = Cu, Ni, H_2), Cu(TBCP), and Cu(IPCP) take one-dimensionally assembled structures and an edge-on configuration at the air-water interface. The Pc's only with alkyl moieties apparantly form a bilayer film at the air-water interface. In contrast, the Pc involving both alkyl and cyano groups can provide a stable monolayer film. This difference arises from the fact that polar cyano groups help to produce a monolayer at the air-water interface despite the symmetrical substitution on the large hydrophobic ring.

§6-7. References

1. Lever, A. B. P. *Adv. Inorg. Chem. Radiochem.* **1965**, *7*, 27.
2. Moser, F. H.;Thomas, A. L. *The Phthalocyanines*; CRC: Boca Raton, FL, 1983.
3. Loutfy, R. O; Sharp, J. H. *J. Chem. Phys.* **1979**, *71*, 1211.
4. Tang, C. W. *Appl. Phys. Lett.* **1982**, *40*, 183.
5. Arishima, K; Hiratsuka, H.; Tate, A.; Okada, T. *Appl. Phys. Lett.* **1985**, *46*, 279.
6. Honeybourne, C. L.; Ewen, R. J.; Hill, C. A. S. *J. Chem. Soc. Faraday Trans. 1.* **1984**, *80*, 851.
7. Sadaoka, Y.; Yamazoe, N.; Seiyama, T. *Denki Kagaku* **1978**, *46*, 597.

8. Moskalev, P. N.; Kirin, I. S. *Rus. J. Phys. Chem.* **1972**, *46*, 1019.
9. Gutierrez, A. R.; Friedrich, J.; Haarer, D.; Wolfman, H. *IBM J. Res. Develop.* **1982**, *26*, 198.
10. *Thin Solid Films* **1985**, Vol. 132-134.
11. Baker, S.; Petty, M. C.; Roberts, G. G.; Twigg, M. V. *Thin Solid Films* **1983**, *99*, 53.
12. Hann, R.A.; Gupta, S. K.; Fryer, J. R.; Eyres, B. L. *Thin Solid Films* **1985**, *134*, 35.
13. Kovacs, G. J.; Vincett, P. S.; Sharp, J. H. *Can. J. Phys.* **1985**, 63, 346.
14. Hua, Y. L.; Roberts, G. G.; Ahmad, M. M.; Petty, M. C.; Hanack, M.; Rein, M. *Phil. Mag. B.* **1986**, *53*, 105.
15. Snow, A. W.; Jarvis, N. L. *J. Am. Chem. Soc.* **1984**, *106*, 4706.
16. Cook, M. J.; Daniel, M. F.; Dunn, A. J.; Gold, A. A.; Thomson, A. J. *J. Chem. Soc. Chem. Commun.* **1986**, 863.
17. Barger, W. R.; Snow, A. W.; Wohltjen, H.; Jarvis, N. L. *Thin Solid Films* **1985**, *133*, 197.
18. Yoneyama, M.; Sugi, M.; Saito, M.; Ikegami, K.; Kuroda, S.; Iizima, S. *Jpn. J. Appl. Phys. Part 1* **1986**, *25*, 961.
19. Baker, S.; Roberts, G. G.; Petty, M. C. *IEE Proc. I.* **1983**, *130*, 260.
20. Snow, A. W.; Barger, W. R.; Klusty, M.; Wohltjen, H.; Jarvis, N. L. *Langmuir* **1986**, *2*, 513.
21. Kalina, D. W.; Crane, S. W. *Thin Solid Films* **1985**, *134*, 109.
22. Fujiki, M.; Tabei, H.; Kurihara, T. *Langmuir* **1988**, *4*, 1123.
23. Fujiki, M.; Tabei, H.; Imamura. S. *Jpn. J. Appl. Phys.Part 1* **1986**, *26*, 1224.
24. Fujiki, M; Tabei, H. *Synth. Met.* **1987**, *18*, 815.
25. Fujiki, M.; Tabei, H. Unpublished results.
26. Sharp, J. H.; Lardon, M. *J. Phys. Chem.* **1968**, *72*, 3230.
27. Sharp, J. H.; Abkowitz, M. *J. Phys. Chem.* **1973**, *77*, 477.
28. Bartolo, B. D., Ed. *Spectroscopy of the Excited State*; Kasha, M.; pp. 337-363; Plenum: New York , N. Y., 1976.
29. Fujiyoshi, Y.; Ueda, N.; Matsumoto, M.; Takenaka, R. 52th National Meeting of the Chemical Society of Japan, Tokyo, April, 1986, Abstr. 1G07.
30. Fryer, J. R.; Hann, R. A.; Eyres, B. L. *Nature* **1985**, *313*, 382.

CHAPTER 7

ELECTRICAL PROPERTIES OF LANGMUIR-BLODGETT FILMS OF PHTHALOCYANINES WITH SHORT ALKYL SUBSTITUENTS

SYNOPSIS

Changes in in-plane conductivities of undoped Langmuir-Blodgett (LB) films of the phthalocyanines containing cyano groups are very fast and highly reversible. The film conductivity increases steeply by five orders of magnitude, when exposed to active gases such as iodine, triethylamine and *n*-butanethiol. Conductivity responses of the LB films to the gases relate to the estimated ionization potentials and electron affinities of the films.

§7-1. Introduction

Phthalocyanines (Pc's) are known to display semiconducting properties.[1-10] Thin films of unsubstituted Pc's are, in general, made by vacuum deposition or dispersion in a polymer binder, because they usually exist in various polymorphic forms and extremely poor solubility in organic solvents. Recently, it has demonstrated that the Langmuir-Blodgett (LB) technique offeres for depositing ultrathin film on solid substrate with desired thickness using of soluble Pc's.[11] Since the report, several workers have studied the preparation, structure and electrical properties on LB films of various suface active Pc derivatives substituted with *tert*-butyl, *iso*-propylaminomethyl, cumylphenoxy groups, and long alkyl chains.[12-23] In order to exploit semiconducting characteristics of Pc's toward microelectronic devices, both the molecular lattice architecture and electronic delocalization of the LB films of Pc's should be controled.

In a first attempt to prepare molecular wires which remain in a highly conducting state without any doping material, we found that thin films of tetrathiafulvalene-tetracyanoquinodimethane, both lacking long alkyl chains, could be formed on hydrophobic substrate using the horizontal lifting LB technique. The maximum conductivity of this films was about 5 $S \cdot cm^{-1}$ at room temperature.[24]

In a second approach, two new soluble NiPc's with four long-chain alkyl amides were found to exhibit one-dimensional self-assembling feature even in dilute solution, and to give bi-axially oriented LB films, as discussed in Chapters 2 - 4. The films showedchanges in conductivity by 2 - 4 orders of magnitude upon iodine vapor exposure. However, since these Pc molecules involves insulating long alkyl chains, electrical conductivity is very low and their electrical response are rather slow.

In this chapter, we describe that ultrathin LB films of soluble Pc's involving short and

compact alkyl and/or cyano groups reveal drastic changes in conductivity under exposure to both electron accepting and donating gases.

§7-2. Experimental

Preparation of lightly substituted Pc's used was fully described in Chapter 5. LB films of the Pc's were deposited on hydrophobic quartz by the horizontal lifting technique at 5 °C of the subphase temperature, as fully described in Chapter 2. Unsubstituted H_2(Pc) LB film was prepared by the reported procedure, in which Li_2(Pc) in acetone is spread on the water-air interface then hydrolyzed *in situ*.[11]

In-plane conductivity of LB films was determined at room temperature from i-v characteristics using a two load dc method with 1 mm separated Au electrodes. Conductivity-time response curves were obtained from a current-time characteristics with a constant bias (10 to 100 volts). All data were collected and analyzed with a HP 4140B pA meter/DC voltage supply with a HP 16055A shield box controlled by a computer. Electrodag 502 was used as a conducting paste.

§7-3. In-Plane Conductivity of Langmuir-Blodgett Films

The orientation of lightly substituted Pc's in LB films as discussed in Chapter 6 suggested that the conductive path of the Pc stack exists parallel to the substrate plane. Therefore, it is interesting to examine in-plane electrical properties.

Table 7-1 summarizes the in-plane conductivity of Pc LB films at room temperature (film thickness; ca. 80 Å). The conductivities of all undoped films ranges from 10^{-8} to 10^{-9} $S \cdot cm^{-1}$. When the films are exposed to iodine vapor (an electron accepting gas), the conductivity increases steeply by 3 - 5 orders of magnitude within a few seconds, finally reaching 10^{-6} to 10^{-3} $S \cdot cm^{-1}$. The LB film of H_2(Pc) shows the highest conductivity among the Pc's. When the undoped films are exposed to triethylamine vapor (an electron donating gas), the film conductivity rapidly increases by 2 - 400 times within a minute. When the undoped films came into contact with *n*-butanethiol (an a donating gas), the film conductivity also increased by 600 - 3000 times within a minute.

The maximum conductivity of LB films of TBP derivatives under exposure to iodine vapor (pressure; ca. 0.5 mmHg) is in the range of $0.3 \cdot 10^{-4}$ to $5 \cdot 10^{-4}$ $S \cdot cm^{-1}$. These values are lower by 1 - 2 orders of magnitude than the conductivity of a polycrystalline pellet of $(TBPSiO)_n$-iodine complex ($2 \cdot 10^{-3}$ $S \cdot cm^{-1}$).[30] This may be attributed to the random orientation of the conducting stacking axes in the substrate plane, since no dichroism is observed in the Q-band region . The maximum conductivities of Cu(TBP) and Cu(TBCP) films exposed to vapors of triethylamine (ca. 60 mmHg) and *n*-butanethiol (ca. 40 mmHg) are ca. $5 \cdot 10^{-6}$ $S \cdot cm^{-1}$. In contrast, Ni(TBP) and H_2(TBP) films show only increases of 2 - 3 times.

Table 7-1. In-Plane Conductivities ($S \cdot cm^{-1}$) of LB Films Prepared by the Horizontal Lifting Technique at Room Temperature.[a]

material	undoped[b]	iodine[c]	triethylamine[d]	*n*-butanethiol[e]
Ni(TBP)	$5.7 \cdot 10^{-8}$	$2.5 \cdot 10^{-4}$	$1.2 \cdot 10^{-7}$	
Cu(TBP)	$1.5 \cdot 10^{-9}$	$3.4 \cdot 10^{-5}$	$1.7 \cdot 10^{-7}$	$5.0 \cdot 10^{-6}$
H_2(TBP)	$3.8 \cdot 10^{-8}$	$5.4 \cdot 10^{-4}$	$1.2 \cdot 10^{-7}$	
Cu(TBCP)	$7.6 \cdot 10^{-9}$	$3.4 \cdot 10^{-4}$	$2.9 \cdot 10^{-6}$	$3.8 \cdot 10^{-6}$
Cu(IPCP)	$4.0 \cdot 10^{-9}$	$4.6 \cdot 10^{-6}$	$8.0 \cdot 10^{-7}$	
H_2(Pc)	$2.9 \cdot 10^{-8}$	$2.6 \cdot 10^{-3}$	$6.0 \cdot 10^{-7}$	

[a] Two stamps were carried out for Ni(TBP), Cu(TBP), H_2(TBP), and H_2(Pc). [b] Four stamps were employed for Cu(TBCP) and Cu(IPCP). Film thickness of these was evaluated to be 80 Å. [c] In air. [d] Vapor pressure was ca. 0.5 mmHg. [e] Vapor pressure was ca. 40 mmHg.

Such differences in the conductivity increment exposed to electron accepting and donating gases might be closely related to the values of ionization potential and electron affinity in thin films.[7]

§7-4. Response in Conductivity Change under Exposure to Active Gases

Figure 7-1 shows changes in the conductivity of Ni(TBP) and Cu(TBCP) LB films as a function of time, when undoped films are first exposed to iodine vapor (ca. 0.5 mmHg) and then to air. When the undoped films are exposed to the gas, the conductivies increase rapidly within a few sec and reach highly conducting states. When the doped films are exposed to air, the conductivity decays at different rates. The conductivity of Cu(TBCP) LB film smoothly returned to the initial value before exposure of iodine vapor within 10 - 30 s. In contrast, although the conductivity of the Ni(TBP) LB film slowly reaches an equilibrium value, the value is 3000 times greater than that in the initial undoped state. The difference of film conductivity change with the kind of electron accepting gases correlates with generation of hole carriers as functions of gas concentration and active site density at the film surface, ionization potential of the film, and electron affinity of gas.[7] The responses of Cu(IPCP) and Cu(TBP) films resemble that of the Cu(TBCP) film. The conductivity responses of the H_2(TBP) and H_2(Pc) LB films are similar to that of the Ni(TBP) film.

Figure 7-2 shows changes in the conductivity of Ni(TBP) and Cu(TBCP) LB films as a function of time when the undoped films are first exposed to triethylamine vapor (ca. 60 mmHg) then to air. When the Cu(TBCP) film is exposed to the gas, the conductivity increases within 20 - 30 s and reaches a fairly conductive state. When the film is then exposed to air, its conductivity returns to the initial value within 20 - 30 s. In contrast, the

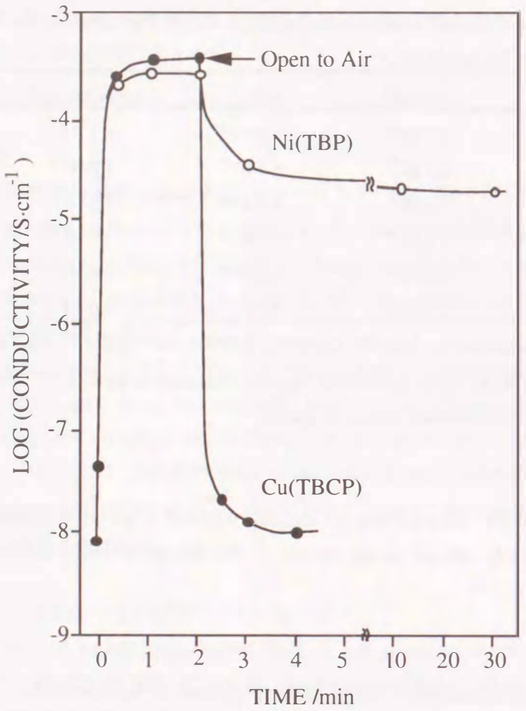

Figure 7-1. Changes in the conductivity of Ni(TBP) and Cu(TBCP) LB films at room temperature when the undoped films are exposed to iodine vapor and then to air. (Vapor pressure; ca. 0.5 mmHg. Film thickness; 80 Å.)

change in conductivity of Ni(TBP) LB film increases only two times when the film is treated with the same way. When undoped Cu(TBP) and Cu(TBCP) LB films are exposed to *n*-butanethiol (a stronger electron donating gas), its saturation conductivity become 2 - 30 times greater than that for triethylamine gas. Such differences in conductivity response to the electron donating gas will be are associated with the generation of electron carriers as functions of gas concentration and active site density at the film surface, electron affinity of the film, and ionization potential of the gas.[7]

Changes in the conductivity of Pc thin films during adsorption or desorption of both electron donating and/or accepting gases have been reported in several Pc thin films.[6,7,19,20,23] The conductivity of the evaporated unsubstituted Cu(Pc) thin film has been reported to increase by one and half orders of magnitude when exposed to NO_2 gas.[6,7] In a

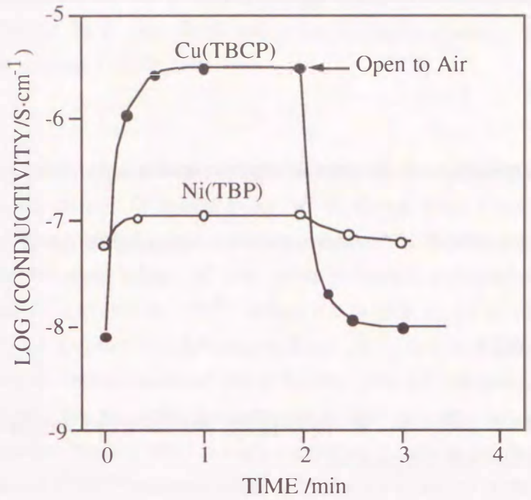

Figure 7-2. Changes in the conductivity of Ni(TBP) and Cu(TBCP) LB films at room temperature when the undoped films are exposed to triethylamine vapor and then to air. (Vapor pressure; ca. 60 mmHg. Film thickness; 80Å.)

series of LB films of M(Pc) (M = H_2, Co, Ni, Cu, Zn, Pd, Pt) with four bulky electron donating cumylphenoxy moieties, the film conductivity increased gradually by 4 orders of magnitude when exposed to iodine vapor and was independent of the complexed central metal ion.[20] These films, however, are unable to return their initial conducting states when exposed to air.[6,7,20] In contrast, an LB film of CuPc which contains three weak electron donating *iso*-propylaminomethyl groups has been shown to change conductivity with introduction and evacuation of NO_2 gas within a few min.[19] These results suggest that the film conductivity is sensitive to the nature of the substituents attached to Pc ring. Ultrathin Pc LB film may correspond to a very active surface layer of the evaporated film or bulk crystals, because of the alignment of the conductive paths of the Pc in the substrate plane and complete interaction with the active gas molecules at the film surface.

§7-5. Theories for Electrical Conductivity[25,26]

A simple expression of electrical dark conductivity, σ, for semiconductors is generally given as,

$$\sigma = n \cdot e \cdot \mu \qquad (7\text{-}1)$$

where n is the carrier density, e the mass of electron and/or hole, and μ the mobility of the carrier.

In the hopping model of free carrier which is applied to the disordered molecular solids, μ is modified as,

$$\mu = e \cdot R^2 \cdot W/kT \qquad (7\text{-}2)$$

where R is the lattice constant, W the hopping probability of the carrier, k Boltzmann constant, and T the absolute temperature.

$$W = \nu \cdot \exp(-\Delta E/kT) \qquad (7\text{-}3)$$

where ν is the frequency of the lattice and ΔE the potential barrier height.

The carrier density in the *n*-type semiconductor, n_d, is given as,

$$n_d = \sqrt{2 \cdot N_d} \cdot (2 \cdot \pi \cdot m \cdot k \cdot T/h^2)^{3/4} \exp\left[\left[-(E_g - E_d)/2 \cdot k \cdot T\right]\right] \qquad (7\text{-}4)$$

where N_d is the density of the donor, h the Planck constant, Eg is the energy gap, E_d the energy level of the donor.

Similarly, the carrier density in the *p*-type semiconductor, n_p, is given as,

$$n_p = \sqrt{2 \cdot N_p} \cdot (2 \cdot \pi \cdot m \cdot k \cdot T/h^2)^{3/4} \exp\left[-(E_p - E_g)/2 \cdot k \cdot T\right] \qquad (7\text{-}5)$$

where N_p is the density of the donor, and E_p the energy level of the acceptor.

In the uniaxial oriented Pc conductors in an LB film, dominant factors in ΔE are the in-plane random orientation, the boundary between the Pc microcrystals, imperfection of Pc array, and defects. These extrinsic problems will diminish the intrinsic mobility of the Pc arrays in the film surface. In contrast, a wide range of the n_d (or n_p) values can vary with the concentration of active gaseous species at the film surface and its electronic potential level. It is expected that the values of ΔE for the six lightly substituted Pc arrays are almost the

same in ultrathin films, since no dichroisms due to in-plane orientation cannot be detected. Accordingly, the difference in the potential energy among the ionization potential and the electron affinity for the the Pc thin films and gaseous species could be the most important factor for electrical responses of the film.

§7-6. Relation Between Electrical Responses and Electronic Potential Parameters

To explain the change in conductivity of the Pc LB film when exposed to active gases, the values of ionization potential and electron affinity of the films should be estimated. Table 7-2 lists the reported values of ionization potential, electron affinity, and redox potential of various Pc derivatives.[7,28-33] When the central metal of the Pc ring changes from Ni, Cu to H_2 in a series of phthalocyanines, TBP, and octacyanophthalocyanines (OCP), the values of ionization potential and reduction potential become positive. When the central metal is Cu and H_2, the reduction potential of TBP becomes negative by about 0.05 eV due to four electron donating alkyl groups compared to that of unsubstituted Pc ring and the reduction potential of OCP becomes positive by *ca.* 1 eV due to eight electron accepting cyano groups.

The values of ionization potential and electron affinity in the Pc LB films are estimated from the following equations.

M(TBP);	$I_P = I_p[M(Pc)] - 0.05$ (eV)	(7-6)
	$E_A = I_p[M(Pc)] - E_g$ (eV)	(7-7)
Cu(TBCP) and Cu(IPCP);	$I_P = I_p[Cu(Pc)] - 0.05 + 1.0/2$ (eV)	(7-8)
	$E_A = I_p[Cu(Pc)] - E_g$ (eV)	(7-9)
H_2(Pc);	$E_A = I_p[H_2(Pc)] - E_g$ (eV)	(7-10)

where I_p is the ionization potential, E_A is the electron affinity, and Eg is the energy gap of the Pc stacks. The transition energy corresponding to λ_{max} values in the LB films are used as the E_g value.

Table 7-3 summarizes the estimated ionization potential and electron affinity values in the present LB systems. The magnitudes of the undoped LB film conductivity are in the rder: Ni(TBP) ≥ H_2(TBP) ≥ H_2(Pc) > Cu(TBCP) ≥ Cu(IPCP) ≥ Cu(TBP). Except for Cu(TBP) this order is consistent with the order of the estimated ionization potential values of the Pc LB films. When these films are doped with iodine vapor, the magnitude of film conductivy become: H_2(Pc) > H_2(TBP) ≥ Cu(TBCP) ≥ Ni(TBP) ≥ Cu(TBP) > Cu(IPCP). However, this order is not consistent with the order of estimated ionization potential values. When the undoped films are treated with triethylamine, the LB film conductivity is in the following order: Cu(TBCP) > Cu(IPCP) ≥ H_2(Pc) > Cu(TBP) ≈ H_2(TBP) ≈ Ni(TBP). This order is consistent with the estimated electron affinity values of the films except for Ni(TBP).

Table 7-2. Previously Reported Values of Redox Potential, Ionization Potential, and Electron Affinity in a series of Phthalocyanine Compounds.

materials	I_P, eV	E_A, eV	E_{oxd}, V (vs SCE)	E_{red}, V (vs SCE)
Ni(Pc)	4.95[a]		1.05[c]	-1.28[d]
Cu(Pc)	5.00,[a] 5.09[b]		0.98[c]	-1.26[d]
H_2(Pc)	5.20[a]		1.10[c]	-1.15[d]
Ni(TBP)				-1.35[e]
Cu(TBP)				-1.31[e]
H_2(TBP)				-1.20[d]
Cu((CN)$_8$Pc))				-0.2[f]
H_2((CN)$_8$Pc))				-0.1[f]
iodine	6.34[g]	4.74[g]		
triethylamine	7.37[h]			

[a] In solid, ref 7. [b] In solid, ref 28. [c] In 1-chloronaphthalene, ref 31. [d] In 1-methylnaphthalene, ref 29. [e] In dichloromethane, ref 30. [f] In dimethylformamide, ref 31. [g] In solid, red 32. [h] In solid, ref 33.

Table 7-3. Estimated Values of Ionization Potential and Electron Affinity in the Pc LB Films Based on Table 7-2 and Equations 7-1 - 7-4.

materials	I_P, eV	E_A, eV
Ni(TBP)	4.90	2.90
Cu(TBP)	4.95	2.85
H_2(TBP)	5.15	3.15
H_2(Pc)	5.20	3.20
Cu(TBCP)	5.45	3.50
Cu(IPCP)	5.45	3.50

Bulky and insulating *tert*-butyl groups would prevent formation of continuous conductive paths in the film plane, since the conductivity of $(TBPSiO)_n$-iodine complex is two orders of magnitude lower than the $(PcSiO)_n$-iodine complex due to the presence of insulating and bulky *tert*-butyl groups.[30] Irreversible response in the conductivity is shown for Ni(TBP), H_2(TBP) and H_2(Pc) LB films when exposed to iodine vapor and then to air. It is possiblethat these Pc molecules tightly form a tight ionic charge-transfer complex with iodine species (eg. I_2, I_3^- or I_5^-) due to lower ionization potential values of the Pc's.[20] High-speed, reversible responses of the LB films conductivity of the Cu(TBCP) and Cu(IPCP) to active gases are advantageous in applications to gas selective sensors, if the ionization potential and electron affinity values of the Pc films can be matched to the detecting gases.

§7-7. Conclusion

The LB film characteristics and the electrical conductivity of several phthalocyanines containing *tert*-butyl, *iso*-propyl, and cyano groups (M(TBP), M(TBCP) and M(IPCP), M=Ni, Cu, Pb and H_2) were examined.

The in-plane conductivity of undoped Pc LB films is in the range of 10^{-8} to 10^{-9} $S \cdot cm^{-1}$. When the films are exposed to iodine vapor (a strong electron acceptor), the conductivity increases by 3000 - 5000 times within a few seconds; the maximum value attained is about $5 \cdot 10^{-4}$ $S \cdot cm^{-1}$. When undoped films are exposed to triethylamine and *n*-butanethiol (electron donors), the initial conductivity increases from 2 - 400 times within 20 to 30 s; the maximum value is $3 \cdot 10^{-6}$ $S \cdot cm^{-1}$. In particular, conductivity changes of Cu(TBCP) and Cu(IPCP) LB films are reversible and highly sensitive, when exposed to accepting and donating gases and then to air. The maximum conductivity and the response of the LB films to the gases correlate with the estimated ionization potential and electron affinity values of the films.

§7-8. References

1. Lever, A. B. P. *Adv. Inorg. Chem. Radiochem.* **1965**, *7*, 27.
2. Moser, F. H.;Thomas, A. L. *The Phthalocyanines*; CRC: Boca Raton, FL, 1983.
3. Loutfy, R. O; Sharp, J. H. *J. Chem. Phys.* **1979**, *71*, 1211.
4. Tang, C. W. *Appl. Phys. Lett.* **1982**, *40*, 183.
5. Arishima, K; Hiratsuka, H.; Tate, A.; Okada, T. *Appl. Phys. Lett.* **1985**, *46*, 279.
6. Honeybourne, C. L.; Ewen, R. J.; Hill, C. A. S. *J. Chem. Soc. Faraday Trans. 1.* **1984**, *80*, 851.
7. Sadaoka, Y.; Yamazoe, N.; Seiyama, T. *Denki Kagaku* **1978**, *46*, 597.
8. Moskalev, P. N.; Kirin, I. S. *Rus. J. Phys. Chem.* **1972**, *46*, 1019.
9. Gutierrez, A. R.; Friedrich, J.; Haarer, D.; Wolfman, H. *IBM J. Res. Develop.* **1982**, *26*, 198.
10. *Thin Solid Films* **1985**, Vol. 132-134.
11. Baker, S.; Petty, M. C.; Roberts, G. G.; Twigg, M. V. *Thin Solid Films* **1983**, *99*, 53.
12. Hann, R.A.; Gupta, S. K.; Fryer, J. R.; Eyres, B. L. *Thin Solid Films* **1985**, *134*, 35.
13. Kovacs, G. J.; Vincett, P. S.; Sharp, J. H. *Can. J. Phys.* **1985**, *63*, 346.
14. Hua, Y. L.; Roberts, G. G.; Ahmad, M. M.; Petty, M. C.; Hanack, M.; Rein, M. *Phil. Mag. B.* **1986**, *53*, 105.
15. Snow, A. W.; Jarvis, N. L. *J. Am. Chem. Soc.* **1984**, *106*, 4706.
16. Cook, M. J.; Daniel, M. F.; Dunn, A. J.; Gold, A. A.; Thomson, A. J. *J. Chem. Soc. Chem. Commun.* **1986**, 863.

17. Barger, W. R.; Snow, A. W.; Wohltjen, H.; Jarvis, N. L. *Thin Solid Films* **1985**, *133*, 197.
18. Yoneyama, M.; Sugi, M.; Saito, M.; Ikegami, K.; Kuroda, S.; Iizima, S. *Jpn. J. Appl. Phys. Part I* **1986**, *25*, 961.
19. Baker, S.; Roberts, G. G.; Petty, M. C. *IEE Proc. I.* **1983**, *130*, 260.
20. Snow, A. W.; Barger, W. R.; Klusty, M.; Wohltjen, H.; Jarvis, N. L. *Langmuir* **1986**, *2*, 513.
21. Kalina, D. W.; Crane, S. W. *Thin Solid Films* **1985**, *134*, 109.
22. Fujiki, M.; Tabei, H.; Kurihara, T. *Langmuir* **1988**, *4*, 1123.
23. Fujiki, M.; Tabei, H.; Imamura. S. *Jpn. J. Appl. Phys. Part I* **1986**, *26*, 1224.
24. Fujiki, M.; Tabei, H. *Synth. Met.* **1987**, *18*, 815.
25. Mikawa, H.; Kusabayashi, S. Eds. In *Kobunshi Handotai (Semiconducting Polymer)*; Kodansha: Tokyo, 1977 [In Japanese].
26. Cox, P. A. *The Electronic Structure and Chemistry of Solids*; Oxford: New York (NY), 1987.
27. Metz, J.; Pawlowski, G.; Hanack, M. *Z. Naturforsch* **1983**, *38B*, 378.
28. Xian, C. S.; Seki, K.; Inokuchi, H., Zurong, S.; Renyuan, Q. *Bull. Chem. Soc. Jpn.* **1983**, *56*, 2565.
29. Campbell, R. H.; Heath, G. A.; Hefter, G. T.; Mcqueen, R. C. S.; *J. Chem. Soc. Chem. Comm.* **1983**, 1123.
30. Louati, A.; El Meray, M.; Andre, J. J.; Simon, J.; Kadish, K. M.; Gross, M.; Giraudeau, A. *Inorg. Chem.* **1985**, *24*, 1175.
31. Wolberg, A.; Manassen, J. *J. Am. Chem. Soc.* **1970**, *92*, 2982.
32. Yamamoto, H.; Seki, K.; Inokuchi, H. *Bunshi Kouzou Tohronkai* 1985, Abstr. No. 2C15, p352.
33. Takahashi, M.; Watanabe, I.; Ikeda, S. *Bunshi Kouzou Tohronkai* 1985, Abstr. No. 3P22, p610.

CHAPTER 8

NEW TETRAPYRROLIC MACROCYCLE: α,β,γ-TRIAZATETRABENZCORROLE

SYNOPSIS

A previously reported divalent germanium phthalocyanine ($PcGe^{II}$) exhibiting unusual electronic and mass spectra when compared with a corresponding high-valent germanium phthalocyanine has been identified as hydroxygermanium α,β,γ-triazatetrabenzcorrole ($TBC^{3-}Ge^{IV}OH$). This identification was achieved by elemental analysis (C, H, N, Ge, and O), spectral measurement (EI- and FD-MS, visible, IR, and ^1H NMR), measurements of chemical reactivity, and oxidative titration. This triazabenzcorrole ring is a new tetrapyrrolic macrocycle. TBCs containing Si, Al, and Ga have also been produced. This ring contractive reaction type of metalloid Pc's occurs generally with introduction of a reductive reagent such as $NaBH_4$ and H_2Se. The molecular symmetry of the TBCGe moiety is exactly C_1 or an approximately 2-fold symmetry showing some distortion.

§8-1. Introduction

Phthalocyanine (Pc) and porphyrin, which are typical macrocycles, are of particular interest in many basic and applied researches concerning catalysts, photoconductors, photosensitizers, models of heme and chlorophyll biosystem, conductive materials, photochemical hole-burning memories, and molecular electronic devices.[1-17] Pc's that contain group IIIA (13) and IVA (14) metalloids, first-low transition metals, and rare-earth metals can provide one-dimensional conductors, whose stacking structures are controlled by covalent linkage (O, F, S, and organic molecules)[11-15] and by the out-of-plane positioning of the central metal.[16,17]

In Chapters 2 - 7, the author discussed the one-dimensionally self-assembled arrays of Pc peripherally substituted with alkylamide, short alkyl, and cyano groups. The fundamental driving forces of such self-assembling features arise from the van der Waals' stacking force of flat Pc rings, directional hydrogen bondings of secondary amides, geometrical shape of short substituents, and symmetrical introduction of these substituents. As a next stage, it is attempted to prepare a one-dimensionally stacked Pc polymer with Ge-Ge spines using divalent germanium Pc ($PcGe^{II}$) in order to achieve higher conductivity.

Recently, Gouterman *et al.*[18,19] reviewed the preparation and electronic spectra of Pc's that contain lower valent metalloids and compared them with those of corresponding higher valent metalloid Pc's. In the review, they pointed out the fact that $PcGe^{II}$ and PcP^{III}

exhibit unusual electronic absorption spectra in contrast to the normal spectra of $PcGe^{IV}$ and PcP^{V}. The Q-bands and B-bands of $PcGe^{II}$ and PcP^{III} are markedly blue-shifted and red-shifted, respectively. They have proposed that the origin of such unusual spectra on PcP^{III} can be attributed to porphyrin-like four orbital electronic transition, which results from closing of the energy gap between a_{1u} (first HOMO) and a_{2u} (second HOMO).[19] In addition, they have suggested from mass spectra data that PcP^{III} has a possibility of having another structure, e.g., $PcPH_2$. However, intense parent mass peak for $PcGe^{II}$ in our preliminary EI- and FD-MS data was detected at m/z 589 ($PcGe^{II}$+3)[20,21] and not at m/z 586 ($PcGe^{II}$) .

In this chapter, the structure of $PcGe^{II}$ was reinvestigated to clarify the cause of this unusual electronic absorption and mass spectra by means of elemental analyses (C, H, N, Ge, and O), IR, visible, FD- and EI-MS, ^1H NMR, and chemical substitution reactions. The present study has concluded that the previously reported $PcGe^{II}$ is not a divalent germanium Pc but a μ-hydroxygermanium^{IV}α,β,γ-triazatetrabenzcorrole (TBCGeOH) formed by the ring contractive reaction of dichlorogermanium^{VI}phthalocyanine.

§8-2. Measurement

Visible and its second derivative visible (2D-visible) absorption spectra were recorded by using a Hitachi 330 double-beam automatic spectrophotometer. Infrared (IR) absorption spectra were recorded with a JASCO 220 double-beam automatic infrared spectrometer. Field desorption ionization mass (FD-MS) spectra were obtained with a Hitachi M-80A mass spectrometer, and electron ionization mass (EI-MS) spectra were obtained by using a JEOL JMS-SG-02 mass spectrometer. A proton nuclear magnetic resonance (^1H NMR) spectrum was recorded with a Hitachi R-600 NMR spectrometer (FT, 60 MHz). A thermal gravimetric diagram (TG) was obtained by using a Rigaku TG apparatus. Elemental analyses for C, H, and N were carried out by using a Heraeus CHN-Rapid automatic elemental analysis instrument and those for Ge and O were performed at the Toray Research Center (Shiga, Japan).

§8-3. Syntheses

(a)Dichlorogermanium^{IV}phthalocyanine ($PcGeCl_2$)

This was prepared by the literature procedure.[22] Anal. Calcd for $C_{32}H_{16}N_8GeCl_2$: C, 58.69; H, 2.46; N, 17.07; Cl, 10.81. Found: C, 58.22; H, 2.34; N, 16.90; Cl, 10.22.

(b)μ-(Benzyloxy)germanium^{IV}α,β,γ-triazatetrabenzcorrole (TBCGeOBz).

A mixture of $PcGeCl_2$ (2.0 g, 3.0 mmol) and $NaBH_4$ (0.37 g, 0.98 mmol) was stirred at 160 °C in a mixture of benzyl alcohol (50 mL) and anisole (25 mL) for 2 h in an Ar gas atmosphere. The hot mixture was filtered under reduced pressure, and anisole in the filtrate

was evaporated under reduced pressure at 100 °C. The residual mixture was then washed with ether, and the resulting solid was repeatedly extracted with hot xylene. Xyrene was evaporated from the dark green extract under reduced pressure at 70 °C. The residue was again washed with ether and dried *in vacuo* for a day at 100 °C. The product was blue fine needles, and the yield was 0.85 g (42%): FD-MS, m/z (rel intensity) 679 (m+, 100), 589 ((M - C_7H_7 + H)+, 100); EI-MS, m/z (rel intensity) 679 (M+, 40), 572 ((M - OCH_2Ph)$^+$, 31), 589 ((M - C_7H_7 + H)$^+$, 7), 1158 ([M - C_7H_7) + (M - OCH_2Ph) - H_2O]$^+$, 100); IR (KBr) ν(CH_2) 2920 w, 2860 w, ν(Ge-O-C) 1040 w; visible ($CHCl_3$) λ_{max} (ε, $M^{-1}cm^{-1}$) 415 ($3.6\cdot10^4$), 442 ($8.0\cdot10^4$), 668 (br, $4.5\cdot10^4$); 2D-visible ($CHCl_3$, Δλ=3nm) λ_{max} (nm) (rel absorbance) 414 (0.13), 424 (0.07), 437 (0.31), 443 (1.00), 607 (0.02), 650 (0.12), 664 (0.08), 676(0.13).

(c)μ-Hydroxygermanium^{IV} α,β,γ-triazatetrabenzcorrole (TBCGeOH).

This compound was identical with previously reported $PcGe^{II}$,[23] as will be discussed later. TBCGeOBz (0.50 g, 0.4 mmol) was refluxed in a mixture of concentrated HCl (10 mL) and ethanol (50 mL) for 10 min. The hot mixture was filtered under reduced pressure and washed with ethanol and then dried *in vacuo* for a day at 100 °C. The product was a dark-green fine needle, and the yield was 0.41g (94 %): FD-MS, m/z (rel intensity) 589 (M^+, 100), 589 ((M - C_7H_7 + H)$^+$, 100); EI-MS, m/z (rel intensity) 589 (M^+, 100), 572 ((M - OH)$^+$, 33), 1158 (2M - H_2O)$^+$, 15); ^1H NMR (D_2SO_4, internal $(CH_3)_4Si$) 9.1 (8H, m, internal H of triazabenzcorrole ring), 10.2 (8H, m, ring external H); IR (KBr) ν(GeO-H) 3250 w, ν(Ge-OH) 718 m; visible (CHCl3) λ_{max} (ε, $M^{-1}cm^{-1}$) 415 ($4.2\cdot10^4$), 444 ($8.7\cdot10^4$), 663 (br, $4.5\cdot10^4$); 2D-visible ($CHCl_3$, Δλ=3nm) λ_{max} (nm) (rel absorbance) 414 (0.15), 424 (0.01), 436 (0.36), 443 (1.00), 649(0.12) 664 (0.15).

(d)μ-Fluorogermanium^{IV} α,β,γ-triazatetrabenzcorrole (TBCGeF).

TBCGeOH (0.40 g, 0.68 mmol) was treated with 50 % HF (50 mL) in a Teflon flask for 2 hr at 60 °C. The product was filtered under reduced pressure and dried in a vacuum for 1 day at 150 °C. The product was dark-blue fine needles, and the yield was 0.38g (100 %): EI-MS, m/z (rel intensity) 591 (M^+, 100), 572 ((M - F)$^+$, 3); IR (KBr) ν(Ge-F) 480 w, ν(Ge-OH) disappearance 718m; visible ($CHCl_3$) λ_{max} (ε, $M^{-1}cm^{-1}$) 415 ($4.1\cdot10^4$), 424 ($8.5\cdot10^4$), 662 (br, $4.5\cdot10^4$); 2D-visible ($CHCl_3$, Δλ=3nm) λ_{max}(nm) (rel absorbance) 414 (0.16), 423 (0.05), 436 (0.34), 442 (1.00), 650 (0.12) 663 (0.11).

(e)μ-Oxobis(germanium^{IV}α,β,γ-triazatetrabenzcorrole) ($(TBCGe)_2O$).

TBCGeOH (10 mg) was heated to 500 °C and then cooled to room temperature in a stream of N_2. This process was monitored with a TG system. A 1.7 % weight loss (theoretical 1.53 %) was observed in the 370 - 410 °C range. The product was dark-blue fine fine needles, and the yield was 9.8 mg (100 %): EI-MS, m/z (rel intensity) 1158 (M^+, 100), 588 ((M - TBCGe)$^+$, 7), 572 ((M -TBCGeO)$^+$, 3); IR (KBr) ν^{as}(Ge-O-Ge) 892s, ν^{s}(Ge-O-

Ge) 867 s, ν(GeO-H) disappearance 3250w, and ν(Ge-OH) disappearance 718m; visible (pyridine) λ_{max}(ε, $M^{-1}cm^{-1}$) 416 ($3.0 \cdot 10^4$), 446 ($8.2 \cdot 10^4$), 661 (br, $4.2 \cdot 10\pm$); 2D-visible (pyridine, $\Delta\lambda$=3nm) λ_{max} (nm) (rel absorbance) 416 (0.20), 437 (0.44), 445 (1.00), 649 (0.12) 664 (0.13).

(f)Trisodium α,β,γ-triazatetrabenzcorrole (TBCNa$_3$(diglyme)$_2$).

A mixture of $PcGeCl_2$ (0.50 g, 0.76 mmol) and $NaBH_4$ (0.10 g, 2.6 mmol) was stirred at 150 °C in diglyme (30 mL) for 2 h in an Ar gas atmosphere. The solvent was evaporated under reduced pressure at 60 °C. The resultant was repeatedly extracted with hot toluene, and the extract was evaporated under reduced pressure at 60 °C. The solid was dried *in vacuo* for 2 days at 60 °C. The product was blue needles, and the yield was 50 mg. EI-MS could not be obtained, due to decomposition: IR (KBr) ν(C-H,diglyme) 2920 m, 2875 m, ν^{as}(C-O-C, diglyme) 1100 br s; visible ($CHCl_3$) λ_{max}(ε, $M^{-1}cm^{-1}$) 416 ($4.6 \cdot 10^4$), 443 ($7.5 \cdot 10^4$), 610 (br, $2.3 \cdot 10^4$), 676 ($8.4 \cdot 10^4$); 2D-visible (CHCl3, $\Delta\lambda$=3nm) λ_{max} (nm) (rel absorbance) 413 (0.27), 422 (0.14), 435 (0.18), 441 (0.60), 451 (0.19), 606 (0.07), 636 (0.06), 650 (0.14), 674 (1.00).

(g)μ-Dihydroxygermanium^{IV}phthalocyanine (PcGe(OH)$_2$).

This was prepared by the literature procedure.[22] Anal. Calcd for $C_{32}H_{18}N_8O_2Ge$: C, 62.08; H, 2.93; N, 21.02. Found: C, 61.888; H, 3.15; N, 20.84. IR (KBr) ν(GeO-H) 3500 s, ν(Ge-OH) 640 s.

(h)Formation of μ-hydroxygermanium^{IV} α,β,γ-triazatetrabenzcorrole from μ-dihydroxy germanium^{IV} phthalocyanine

$PcGeCl_2$ (0.32 g, 0.52 mmol) was allowed to react in quinoline (40 mL) for 10 min at room temperature, for 20 min at 100 °C, for 20 min at 120 °C, for 4 h at 160 °C, during which H_2Se/Ar (50/50 wt %) gas was bubbled in. The hot reaction mixture was filtered, and the filtrate was allowed to cool for 2 days. The precipitate was filtered under reduced pressure and washed with ethanol and acetone and then dried in a vacuum for a day at 100 °C. The product was identified as TBCGeOH from elemental analyses (C, H, and N), IR and visible spectra.

§8-4. Re-Characterization of Germanium^{II}phthalocyanine and Identification of μ-Hydroxygermanium^{IV}α,β,γ-triazatetrabenzcorrole

Joyner *et al.*[23] concluded from elemental analyses (C, H, and Ge), IR and UV-visible absorption spectra, and oxidative analysis of the central metal that the reduction product of $PcGeCl_2$ with $NaBH_4$ was PcGe^{II}.[24] Because PcGe^{II} exhibits unusual electronic absorption

Table 8-1. Results of Elemental Analysis on Triazatetrabenzcorrole Derivatives.

compound	found(%)					calcd(%)				
	C	H	N	Ge	O	C	H	N	Ge	O
TBCGeOH	65.50	2.85	16.15	13.05	3.70	65.36	2.91	16.66	12.34	2.72
PcGe^{II} [a]	65.86	2.91		12.63		65.39	2.76	19.14	12.41	0.00
TBCGeOBz	69.33	3.30	14.77		3.15	69.07	3.42	14.45		2.36
TBCGeF·0.5H_2O	63.90	2.85	16.04			64.15	2.86	16.35		
(TBCGe)$_2$O	66.85	2.65	16.63		1.64	66.38	2.79	16.92		1.38
TBCNa·(diglyme)$_2$	62.29	4.98	11.60		12.82	63.23	5.31	11.73		11.49

[a] Note data from ref 23.

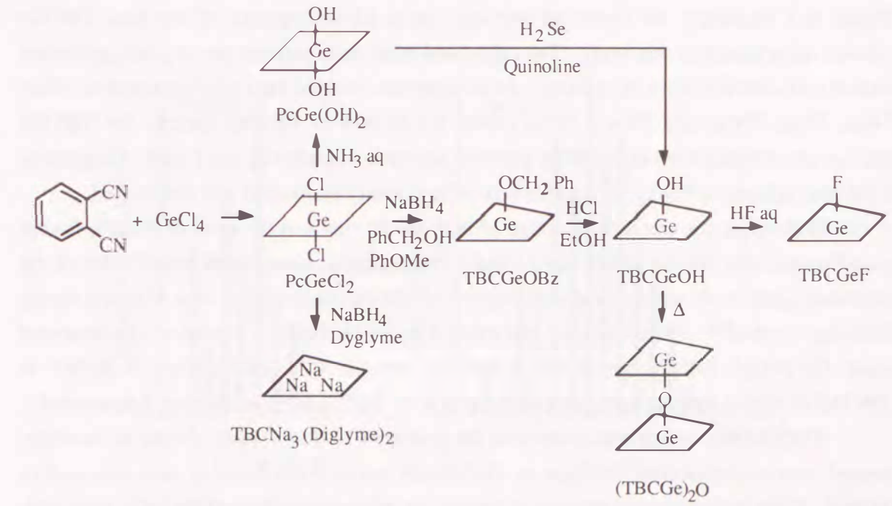

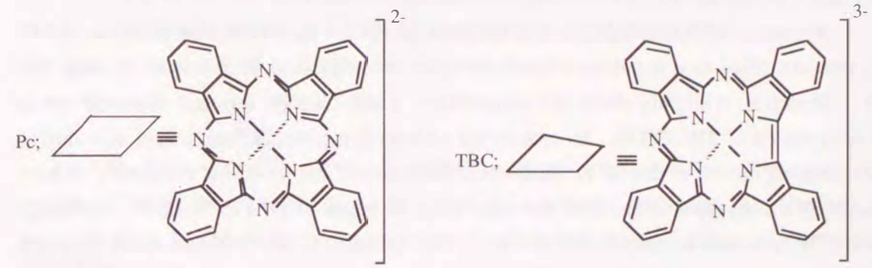

Figure 8-1. Synthetic scheme of α,β,γ-triazabenzcorrole derivatives from *o*-phthalonitlile as starting matrial.

spectra in contrast to the normal spectra of $PcGe^{IV}$, the chemical structure of $PcGe^{II}$ was reinvestigated by elemental analyses (C, H, N, Ge, and O), IR, visible, FD- and EI-MS, ^1H NMR, and chemical reactions. Based on the following evidences, $PcGe^{II}$ is identified not to be a divalent germanium Pc but a μ-hydroxygermanium^{IV}α,β,γ-triazatetrabenzcorrole (TBCGeOH) which is new tetrapyrrolic macrocycle.

Table 8-1 gives the results of elemental analyses for the five triazabenzcorrole derivatives. The observed values are in good agreement with the calculated values of the corresponding triazabenzcorrole derivatives. The observes values of C, H, and Ge for TBCGeOH are consistent with the calculated values for both TBCGeOH and $PcGe^{II}$. However, only 7 atoms of N are observed, whereas there are 1.4 atoms of O. The extra 0.4 atoms of O may be due to an inaccuracy in the CO reduction method.

Figure 8-1 illustrates the synthetic scheme of triazatetrabenzcorrole derivatives. Figure 8-2 illustrates the observed and calculated EI-MS spectra of the four TBCGe derivatives prepared in this study. The calculated mass peak patterns are in good agreement with the observed results, by taking into account the isotopic natural abundance of ^{70}Ge, ^{72}Ge, ^{73}Ge, ^{74}Ge, and ^{76}Ge. From either the EI-MS or FD-MS spectra for TBCGe derivatives, the expected elimination patterns for these compounds are found. Especially, either the hydroxy or benzyl group attached to Ge is easily eliminated and dehydrated.

With respect to the formal charge of both the Pc ring and Ge atom in $PcGe^{II}$, Joyner *et al.*[23] concluded that Ge and Pc are 2+ and 2-, respectively, since the observed value of the oxidation agent/mole was in close agreement with the calculated value of it obtained by the Eldvidge method[24]: obsd 3.1 equiv and calcd 4 equiv for $PcGe^{II}$. However, the observed value for $PcGe^{II}$ fully supports the calculated one for TBCGeOH, since if $PcGe^{II}$ is TBCGeOH with a formal charge of $TBC^{3-}Ge^{4+}OH^{1-}$, TBCGeOH should have 3 equiv/mol.

TBCGeOBz, which was isolated as the precursor of TBCGeOH, should be carefully treated, since TBCGeOBz resulted in TBCGeOH easily even when it was refluxed in ethanol. Since Joyner *et al.*[23] previously treated the reduction product of $PcGeCl_2$ with acid, the crude TBCGeOBz might be converted to TBCGeOH ($PcGe^{II}$).

Joyner *et al.*[23] also reported that the purified $PcGe^{II}$ by sublimation *in vacuo* at 357 °C, was identified as a β-polymorphism, showing the additional IR bands at 887 and 860 cm^{-1}. However, at slightly above this temperature, a small weight loss was observed due to he dehydration of TBCGeOH. Moreover, the additional intense IR bands were seen due to the stretching modes of the Ge-O-Ge bonds at 892 and 867 cm^{-1}. This is concurrent with be caused by the disappearance of the corresponding IR bands of the GeOH bond. Similarly, $PcGe(OH)_2$ which is dehydrated at 340 - 380 °C leads to an O-linked PcGe polymer ($(PcGe)_n$) with intense IR bands at 887 and 860 cm^{-1} which should be assigned as the Ge-O-Ge bonds and not the β-polymorphism. It is thought that the sublimed $PcGe^{II}$ partially included $(TBCGe)_2O$.

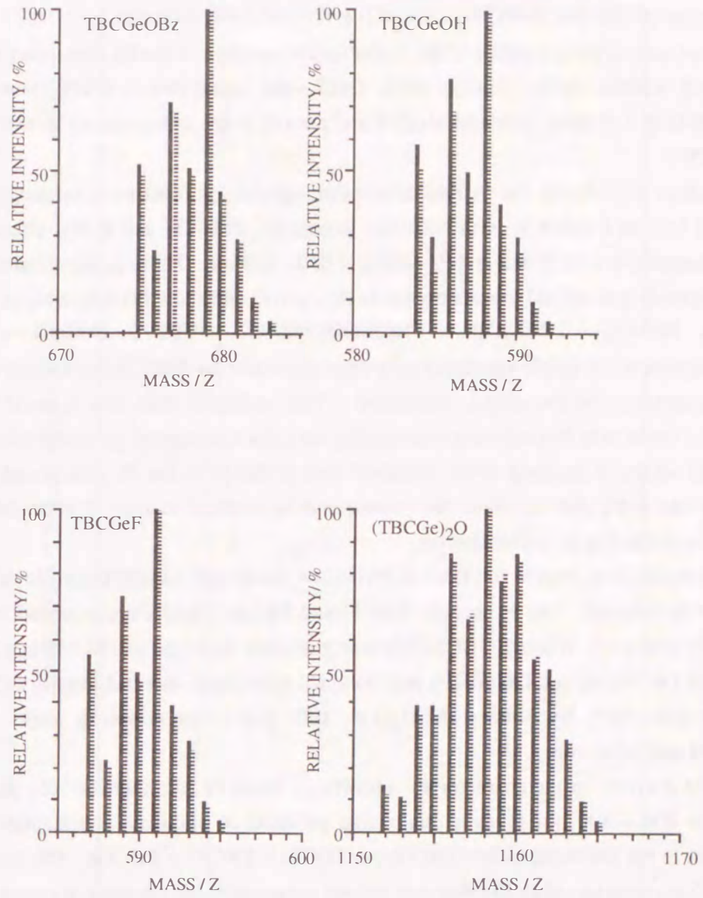

Figure 8-2. Observed (solid line) and calculated (dotted line) EI-MS spectra for germanium^{IV}α,β,γ-triazatetrabenzcorrole derivatives.

$PcGe(OH)_2$ were also converted to TBCGeOH by treatment with an H_2Se gas. The purpose of this reaction was to obtain a Se-linked PcGe polymer, $(PcGeSe)_n$, like $(PcGeS)_n$[13] for application to one-dimensional conductors. Although no $(PcGeSe)_n$ was obtained, $PcGe(OH)_2$ undergoes a contractive reaction of the Pc ring due to the elimination of a bridged N in Pc ring with an H_2Se gas.

§8-5. Characterization of Other Metalloid α,β,γ-Triazatetrabenzcorroles

To examine the generality of these contractive reaction of the Pc ring, other metalloid Pc's which contain $SiCl_2$, $SnCl_2$, AlCl, GaCl, and metal-free Pc (PcH_2) were reacted with $NaBH_4$ in a mixture of benzyl alcohol and anisole in the same manner as that used for TBCGeOBz.

Figure 8-3 shows the visible absorption spectra of reaction mixtures for these metalloid Pc's and $PcGeCl_2$ with $NaBH_4$. Except for $PcSnCl_2$ and PcH_2, characteristic visible absorptions were found at 440 - 450 and 650 - 680 nm. These peaks are attributed to the corresponding metalloid triazabenzcorrole derivatives and show the following contractive reactions: $PcSiCl_2 \rightarrow$ TBCSiOBz or TBCSiOH, PcAlCl → TBCAl, PcGaCl → TBCGa. This is because these visible spectra closely resemble those for TBCGe derivatives and have some dependence on the central metalloid. This indicates that this type of the ring contractive reaction in Pc compounds containing the reductive reagent generally occurs when both of Cl which is attached to the metalloid and bridge N in the Pc ring are eliminated. $PcSnCl_2$ and PcH_2 did not show the corresponding absorption spectra characteristic of triazabenzcorrole ring in visible spectra.

Unfortunately, except for TBCGe derivative, metalloid triazabenzcorrole derivatives could not be isolated. This is because TBCAl and TBCGa rapidly decomposed in contact with water and/or air. Though TBCSiOBz was gradually decomposed, EI-MS spectrum for unpurified TBCSiOBz (or TBCSiOH) was obtained as follows: m/z (rel intensity) 543 (M^+, 59), 526 ($(M\text{-}OH)^+$, 6), 1068 ($(2M\text{-}H_2O)^+$, 100) and other coupling peaks between TBCSiOH and $PcSi(OBz)_2$.

The decrease in the characteristic absorption bands of triazabenzcorrole ring in wet ethanol at 400 - 500 nm gives a qualitative estimate of stability of triazabenzcorrole derivatives in the following order: TBCGe >> TBCSi > TBCAl > TBCGa. The reason why only TBCGe could be stably isolated may be due to the fit of the covalent or cationic radius of the central metalloids and the internal hole radius of the triazabenzcorrole ring. Only Ge appears to satisfy the precise size requirement to fit into the internal hole of triazabenzcorrole ring. The covalent and cationic radii for various metalloids are listed as follows:[27] Si (1.17 Å), Ge (1.22 Å), Sn (1.40 Å); and Si^{IV} (0.54 Å), Ge^{IV} (0.54 Å), Sn^{IV} (0.71 Å), Al^{III} (0.45 Å), Ga^{III} (0.60 Å).

PcP^{III}, which exhibits unusual electronic absorption and mass spectra,[18,19] may have actually the $TBCP^{V}$=O structure. The oxygen in $TBCP^{V}$=O may arise from water and/or air. This is because the UV-visible absorption spectra of PcP^{III} closely resemble that of TBCGeOH ($PcGe^{II}$) and the observed MS parent peak for $(PcP^{III} + 2)^+$ (m/z 545.5) is consistent with the calculated value for $(TBCP^{V}=O)^+$ (m/z 545).

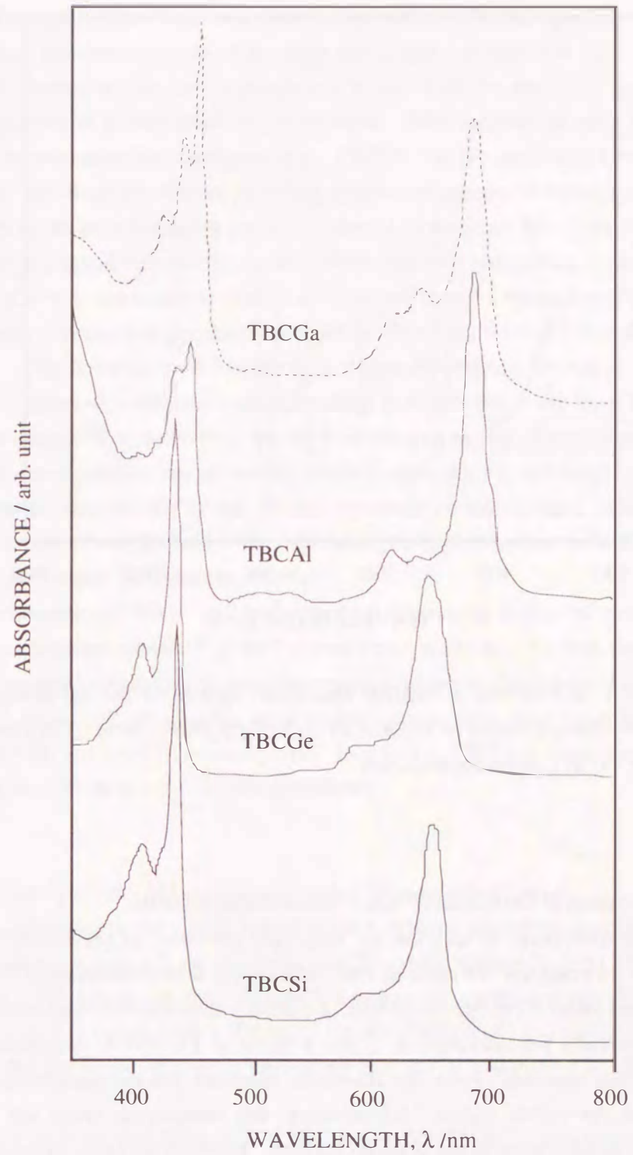

Figure 8-3. Visible absorption spectra of metalloid triazabenzcorrole derivatives (measuring solvent: *iso*-propyl alcohol, room temperature).

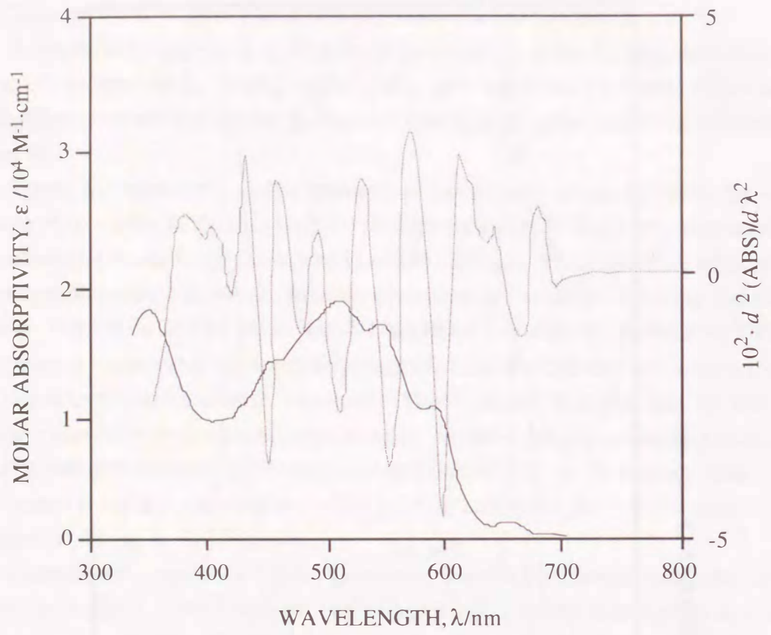

Figure 8-4. Visible and 2D-visible absorption spectra of the red compound formed by decomposition of TBCGeOH under light illumination ($[TBCGeOH]_0$ = $2.5 \cdot 10^{-5}$ M in 1-chloronaphthalene).

§8-6. Decomposition of Germanium^{IV} α,β,γ-Triazatetrabenzcorrole

TBCGe derivatives in solution are very light sensitive, as previously reported by Joyner *et al.*[23] In examples, the color of TBCGeOH in dilute solution changes from green to red when placed under room light overnight. Figure 8-4 shows the visible spectra of the red solution. Apparently the characteristic Q and B bands of TBCGeOH disappeared, and the new, broad bands appeared. From the 2D-visible spectrum, the red compound has at least eight bands in the visible region. Unfortunately, this compounds could not be isolated because of strong adsorption to the silica gel column. Although the exact chemical structure of the red compound is not clear, it may be a ring cleavage or ring expansion compound of the TBCGeOH, as would be expected from the chemical or photochemical reactivity of the 1-2 position of triazabenzcorrole ring. (See Figure 8-1.) Predicted structures of the red compound are shown in Figure 8-5.

§8-7. Ring Contractive Reaction Mechanism of Germanium^{VI} Phthalocyanine

The fact that extremely stable Pc rings easily lose a bridge N is quite unusual. To explain this novelty, we propose a possible scheme of the Pc ring contraction reaction although experimetal confirmation is yet to come. This mechanism may help the new syntheses of triazabenzcorrole analogues, e.g., TBCCo, TBCFe, and TBCCr.

Figure 8-6 illustrates the reductive ring contraction scheme of $PcGeCl_2$ with $NaBH_4$. The first step shows the elimination process of two Cl atomes from Ge. This is based on the fact that only metalloid Pc's containing Cl lead to the ring contraction reaction. Next, $(Pc^{2-})(Ge^{4+})(Cl^{1-})_2$ is converted to $(Pc^{2-})(Ge^{2+})$, which changes immediately $(Pc^{4+})(Ge^{4+})$, through a intramolecular charge-transfer reaction from the $4P_z$ level of Ge to the e_g level of the Pc ring. This is because $(Pc^{2-})(Ge^{2+})$ is thermodynamically unstable. $(Pc^{4-})(Ge^{4+})$ cannot hold a planer structure and lead to bending of the Pc ring along the a-b axis, which includes two bridged N of the Pc ring, arising from the spin pairing of two electrons in the e_g level. These intramolecular charge-transfer reaction, spin-pairing, and bending of the (Pc^{4-}) ring are supported theoretically by our preliminary results on the extended Hückel molecular orbital calculation. Then, the bridge N of the bend $(Pc^{4-})(Ge^{4+})$ reacts with BH_4^- (or BH_3) and eliminated. Finally, TBCGeOBz is formed.

The chemistry of TBC^{3-} will be interesting concerning biological models, such as vitamine B_{12} coenzyme models,[28] as well as conductive materials. To date, there have been no synthetic reports on triazabenzcorrole macrocycles which are homologues of corrole ring compounds. As is well-known, Pc's without side groups have poor solubility in organic solvents (10^{-4} M) and exhibit polymorphism. In contrast, TBC ring have good solubilities (TBCGeOH, ca. 10^{-2} M in hot 1-chloronaphthalene).

§8-8. Molecular Symmetry of Germanium^{IV} α,β,γ-Triazatetrabenzcorrole

The differences in the visible and IR spectra between triazabenzcorrole and Pc rings have been studied. Figure 8-7 shows visible and 2D-visible spectra for both TBCGeOH and $PcGeCl_2$ in 1-chloronaphthalene. Figure 8-8 shows IR absorption spectra in the ring deformation (ϕ(C-C)) region (400 - 700 cm^{-1}) for both TBCGeOH and $PcGeCl_2$. Table 8-2 summarizes the electronic absorption parameters and partial assignment in TBCGeOH and $PcGeCl_2$.

From Figure 8-7 and Table 8-2, it can be seen that $PcGeCl_2$ possesses a degenerate and sharp Q(0' - 0") band at 14310 cm^{-1}, which is assigned to the allowed ($e_g \leftarrow a_{1u}$), and additional weak vibrational bands (0'-1", 0'-2"). It also has broad and intense B bands (Soret band), which are assigned to the allowed transition ($e_g \leftarrow a_{2u}$). These electronic absorption spectra of $PcGeCl_2$ are consistent with molecular symmetry of D_{4h}.[2]

Table 8-2. Electronic Absorption Parameters and Tentative Assignment of μ-Hydroxy-germanium^{IV}α,β,γ-Triazatetrabenzcorrole and Dichlorogermanium^{IV} Phthalocyanine.

compounds	E,[a] cm^{-1}	A[b]	ε,[c] $M^{-1}\cdot cm^{-1}$	f,[d] erg·cm
TBCGeOH (C_1)	14820	$Q_1(0'\text{-}0'')$		
	14950	$Q_2(0'\text{-}0'')$	$5.1\cdot10^4$	0.09
	15250	$Q_3(0'\text{-}0'')$		
	22270	$B_1(0'\text{-}0'')$	$8.9\cdot10^4$	
	22620	$B_2(0'\text{-}0'')$		0.31
	23830	$B_3(0'\text{-}0'')$	$4.4\cdot10^4$	
$PcGeCl_2$ (D_{4h})	14310	$Q(0'\text{-}0'')$ ($e_g \leftarrow a_{1u}$)	$2.6\cdot10^5$	0.23
	27300	$B(e_g \leftarrow a_{2u})$	$7.3\cdot10^4$	0.59

[a]Note E is the electronic transition energy. [b]A is the assignments for the electronic transition. [c]ε the molar absorption coefficient per liter. [d]f the oscillator strength. All measurement were carried out in 1-chloronaphthalene at room temperature.

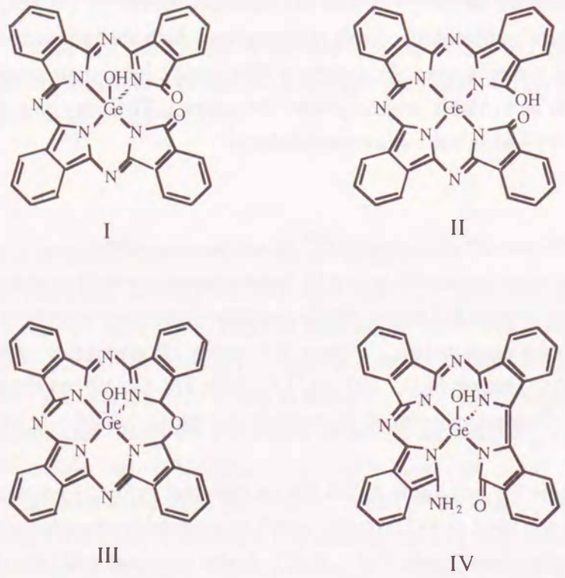

Figure 8-5. Four possible chemical structures of the red colored compound produced by decomposition of μ-hydroxygermanium^{IV} α,β,γ-triazatetrabenzcorrole under room light irradiation.

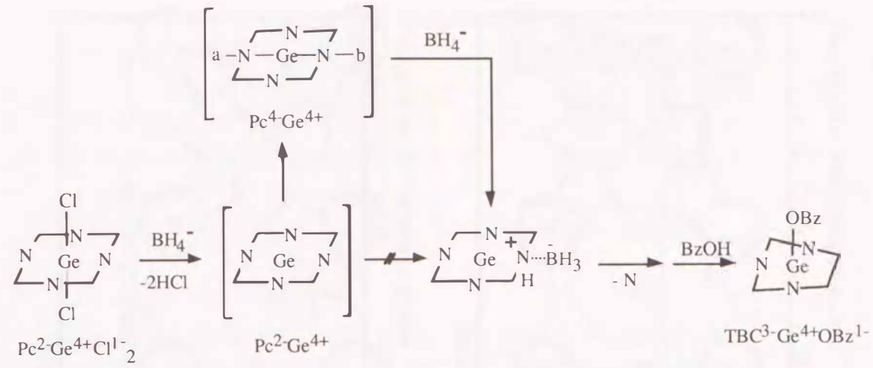

Figure 8-6. Proposed scheme of the Pc ring contraction reaction for the $PcGeCl_2$-$NaBH_4$ system. (N means the bridged N of the Pc or triazabenzcorrole ring. The a-b in $Pc^{4-}Ge^{4+}$ stands for a folding axis of Pc ring.)

On the other hand, although from normal visible spectrum TBCGeOH has two characteristic Q and B bands near 450 and 660 nm, both Q(0'-0") and B(0'-0") bands from 2D-visible spectrum are more complex, as would be expected that the symmetry of TBCGeOH is necessarily reduced from D_{4h} to C_{2h}. Such splitting of the electronic absorption spectra arises from the splitting of the degenerate first LUMO (e_g) of Pc with D_{4h} symmetry.[2]

In Table 8-2, electronic absorption parameters and partial assignment of TBCGeOH and $PcGeCl_2$ is listed. The oscillator strengths (f) of Q and B bands of TBCGeOH are found to be only 40 - 50 % of the corresponding strengths for $PcGeCl_2$. The decrease in f may indicate a lack of planarity in TBCGeOH.

From Figure 8-8, we can see that in ϕ(C-C) region, $PcGeCl_2$ has four characteristic peaks that result from the Pc ring structure with D_{4h} molecular symmetry,[29] while TBCGeOH has eight peaks. The splitting of the ϕ(C-C) peaks of the macrocycles is as follows: $PcGeCl_2 \rightarrow$TBCGeOH, ϕ(C-C)(cm^{-1}); 430 → 410 + 445, 509 → 522 + 538, 570 → 572 + 580, 640 → 628 + 650. This splitting of ϕ(C-C) peaks can also be explained as a result of the decrease in the molecular symmetry of the triazabenzcorrole ring.

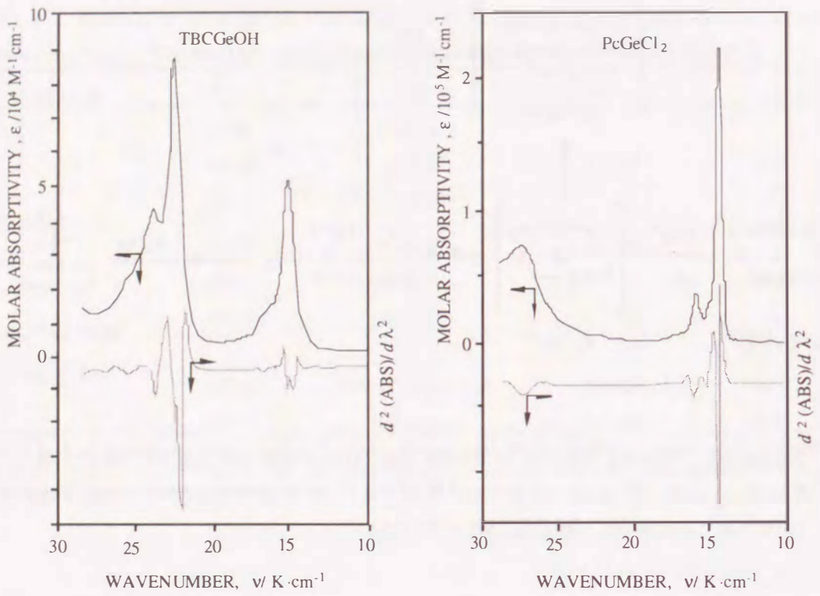

Figure 8-7. Visible and 2D-visible absorption spectra for μ-hydroxy-germanium ^{IV}α,β,γ - triazatetrabenzcorrole and dichlorogermanium ^{IV}phthalocyanine in 1-chloronaphthalene at room temperature.

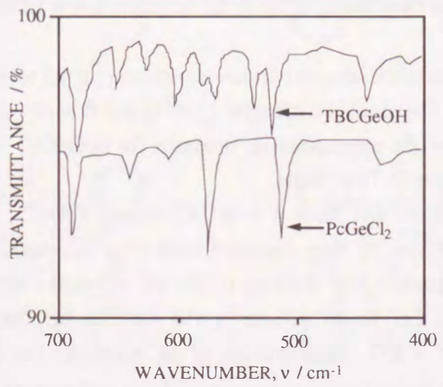

Figure 8-8. IR transmittance spectra of μ-hydroxygermanium^{IV}α,β,γ-triazatetrabenzcorrole and dichlorogermanium^{IV}phthalocyanine in KBr.

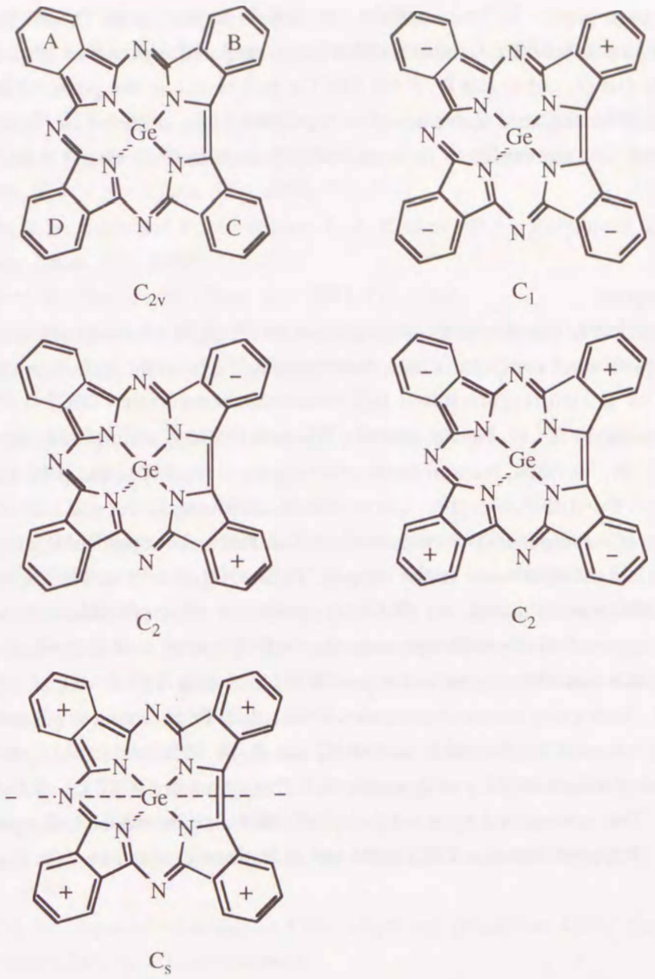

Figure 8-9. Proposed molecular structural models for the germanium^{IV}α,β,γ-triazatetrabenzcorrole moiety.

Thus, the visible and IR spectra indicate that the molecular symmetry of the triazabenzcorrole ring has dropped from 4-fold to 2-fold. There may be also additional distortion from C_{2v} to C_2, C_s, or C_1. Indeed, a CPK space filling model of TBCGeOH cannot have a planer structure of a TBCGe moiety. Figure 8-9 shows proposed structural models for a TBCGe moiety, where + indicates displacement above the page plane and -

below the page plane. In four adjacent isoindoline planes (A, B, C, and D), the steric hindrance of a pair between A and B is rather large compared with that of other pairs such as A and C, B and D, and C and D, if the TBCGe moiety lies in the plane. Therefore, this moiety should be displaced above or below the GeN4 plane, as shown in Figure 8-9. Such distortion has been reported even for such Pc compounds as $(PcSnO)_n$,[29] PcPb,[30] and $PcK_2(diglyme)_2$.[31]

§8-9. Conclusion

A previously reported divalent germanium Pc ($PcGe^{II}$), which showed unusual visible and MS spectra when compared with a corresponding high-valent germanium Pc, has been identified as μ-hydroxygermanium α,β,γ-triazatetrabenzcorrole ($TBC^{3-}Ge^{IV}OH$) from elemental analyses (C, H, N, Ge, and O), EI- and FD-MS, visible (normal and second differential), IR, ^1H NMR, measurements of its chemical reactivity, and previously reported results. From the visible absorption spectra, TBCs containing Si, Al, and Ga were produced in a mixture of corresponding chlorinated metalloid Pc's and sodium borohydride and were found to be less stable to water and/or oxygen. $PcGe(OH)_2$ results in TBCGeOH following H_2Se gas treatment, although no $(PcGeSe)_n$ polymers were obtained. In addition, the previously reported trivalent phosphorous Pc (PcP^{III}) which was also reported to have unusual visible and MS spectra has a possibility of being $TBCP^{V}=O$, in analogy with TBCGeOH. Such a ring contractive reaction of metalloid Pc's is found to generally occur by introducing reductive reagents such as $NaBH_4$ and H_2Se. The molecular symmetry of the TBCGe moiety was exactly C_1 or approximate 2-fold symmetry (C_{2v}, C_2, or C_s) with some distortions. This is supported by its solubility, a CPK molecular model, and a comparison of visible and IR spectra between TBCGeOH and dichlorogermanium Pc with D_{4h} molecular symmetry.

§8-10. References

1. Melson, G. A., Ed. *Coordination Chemistry of Macrocyclic Compounds* ; Plenum: New York, NY, 1979.
2. Lever, A. B. P. *Adv. Inorg. Chem. Radiochem*. **1965**, *7*, 27.
3. Dolphin, D., Ed. *The Porphyrins* ; Academic: New York, NY, 1978; Vol. 1-10.
4. Moser, F. H.; Thomas, A. L. *The Phthalocyanines* ; CRC: Boca Raton, FL, 1983.
5. Smith, K. M., Ed. *Porphyrins and Metalloporphyrins* ; Elsevier: Amsterdam, 1975.
6. Miller, J. S., Ed. *Extended Linear Chain Compound* ; Plenum: New York, NY, 1982; Vols. 1-3.
7. Loutfy, R. O., *Phys. Status Solidi A* **1981**, *A65*, 659.
8. Loutfy, R. O.; Sharp, J. H. *J. Chem. Phys.* **1979**, *71*, 1211.
9. Gutierrez, A. R.; Friedrich, J.; Haarer, D.; Wolfman, H. *IBM J. Res. Develop.* **1982**, *26*, 198.
10. Carter, F. L., Ed. *Molecular Electronic Devices*; Dekker; New York, NY, 1982.
11. Diel, B. N.; Inabe, T.; Lyding, J. W.; Schoch, K. F. Jr.; Kannewurf, C. R.; Marks, T. J. *J. Am. Chem. Soc.* **1983**, *105*, 1551.
12. Nohr, R. S.; Kuznesof, P. M.; Wynne, K. J.; Kenney, M. E.; Siebenman, P. G. *J. Am. Chem. Soc*. **1981**, *103*, 4371.
13. Fischer, K.; Hanack, M. *Chem. Ber.* **1983**, *116*, 1860.
14. Diel, B. N.; Inabe, T.; Jaggi, N. K.; Lyding, J. W.; Schneider, O.; Hanack, M.; Kannewurf, C. R.; Marks, T. J.; Schwartz, L. H. *J. Am. Chem. Soc.* **1984**, *106,* 3207.
15. Hanack, M.; Mitulla, K.; Pawlowsky, G.; Subramanian, L. R. *J. Organomet. Chem.* **1981**, *204*, 315.
16. Ukei, K. *J. Phys. Soc. Jpn.* **1976**, *40*, 140.
17. Yamana, M.; Tsutsui, M.; Ham, J. S. *J. Chem. Soc.* **1982**, 76, 2761.
18. Sayer, P.; Gouterman, M.; Connell, C. R. *Acc. Chem. Res.* **1982**, *20*, 87.
19. Gouterman, M.; Sayer, P.; Shankland, E.; Smith, J. P. *Inorg. Chem.* **1981**, *20*, 87.
20. Isa, K.; Sasaki, K.; Mizuta, K.; *Shituryou Bunseki* **1984**, *32*, 305.
21. Fujiki, M.; Mori, Y.; Tabei, H. *47th National Meeting of the Chemical Society of Japan*, Kyoto, April, 1983, Abstr. 2B11.
22. Joyner, R. D.; Kenney, M. E. *J. Am. Chem. Soc.* **1960**, *82*, 5790.
23. Stover, R. L.; Thrall, C. L.; Joyner, R. D. *Inorg. Chem.* **1972**, *10*, 2335.
24. Elvidge, J. A. *J. Chem. Soc.* **1961**, 869.
25. Dirk, C. W.; Inabe, T.; Schoch, K. F. Jr.; Marks, T. J. *J. Am. Chem. Soc.* **1983**, *105*, 1539.
26. Fujiki, M. Unpublished results. A 4.9% weight loss (theoritical 2.9%) was observed for $PcGe(OH)_2$ by TG measurement.
27. Cotton, F. A.; Wilkinson, G. *Advanced Inorganic Chemistry*, 2nd ed.; Wiley: New York, NY, 1966.
28. Murakami, Y.; Aoyama, Y.; Tokunaga, K. *J. Am. Chem. Soc.* **1980**, *102*, 6736.
29. Stymne, B.; Sauvage, F. X.; Wettermark, Q. *Spectrochim. Acta* **1979**, *35A*, 1195.
30. Ukei, K. *Acta Crystallogr.* **1973**, *B29*, 2290.
31. Ziolo, R. F.; Gunther, W. H. H.; Troup, J. M. *J. Am. Chem. Soc.* **1981**, *103*, 4629.

CHAPTER 9

CONCLUDING REMARKS

Main subjects of the present thesis are to construct one-dimensional phthalocyanine self-assembling structures and to control its conductivity in the Langmuir-Blodgett film. The following results obtained in the study will provide an avenue to explore potential application for practical uses. The author hopes that the present study will be a fingerpost for the future direction in the research of phthalocyanine-based conductors.

[1] Two new types of highly soluble nickel phthalocyanines containing four octadecylamides (AmPc1 and AmPc2) are prepared. Both the AmPc1 and AmPc2 derivatives are predicted to form one-dimensional, self-assembled structures with van der Waals' thickness. This results from the hydrogen-bonding force of the secondary amides in the solid, in the cast films, and in the solutions and is evident from the visible and emission spectra and the X-ray diffraction data. The assembling numbers in AmPc1 and AmPc2, which strongly depend on the condition of the solution, are evaluated as 5 - 18 for AmPc1 and 2 - 5 for AmPc2 using a modified molecular exciton theory.

[2] Langmuir-Blodgett (LB) films of soluble nickel phthalocyanines with four octadecylamide substituents (AmPc1 and AmPc2) are studied. The films have been prepared by both the vertical dipping and horizontal lifting techniques. The assembling numbers of AmPc1 and AmPc2 in the LB films strongly depend on the preparation conditions of the LB films, and evaluated as ca. 5 - 14 for the AmPc1 and 5 for the AmPc2 using a modified molecular exciton theory. In-plane dichroisms can be invariably seen in UV-visible and IR regions for the LB films prepared by either the vertical dipping or horizontal lifting technique. The dichroic ratios are sensitive to the conditions of film preparation (film pressures, transfer rates of substrates, additives, and film transfer techniques). Molecular arrangement and orientation in the AmPc1 LB film prepared by the vertical dipping method are characterized by means of the polarized UV-visible and IR spectra, and force-area isotherm.

[3] Patterning and electrical properties of these LB films (AmPc1 and AmPc2) are examined. The films are prepared by the LB and spin cast techniques. The film conductivities increase by 2 - 4 orders of magnitude upon iodine vapor exposure up to the value of ca. 10^{-6} $S \cdot cm^{-1}$. Both the AmPc1 and AmPc2 thin films show negative patterning feature to electron beam (EB) dose, and excellent resistance to plasma assisted dry etching.

AmPc2 possesses high contrast value in the LB film ($\gamma = 3.8$) and high reactivity ($D_0 = 3.5$ $\mu C \cdot cm^{-2}$) in the spin cast film. The fine patterns are fabricated in the AmPc2 spin cast film down to lines of width 0.8 μm with 0.8 μm spacing using EB irradiation and wet etching. The semiconducting properties of the Pc ring moieties are possibly maintained without decomposition of Pc ring structure during the fabrication process.

[4] Several tetra(*tert*-butyl)phthalocyanine derivatives are prepared. Also, two new types of metallophthalocyanines containing both alkyl (*tert*-butyl or *iso*-propyl) and cyano groups are obtained successfully. These compounds are prepared from alkylbenzenes in only two or three steps with excellent yields. A previous synthetic method for tetra(*tert*-butyl)phthalocyanines required seven steps from *o*-xylene. ^1H NMR spectra and high performance liquid chromatogram indicate the presence of three of its four possible geometric isomers. Reaction mechanisms of these phthalocyanines are also discussed.

[5] The molecular arrangement and orientation of phthalocyanine molecule in LB films of several phthalocyanines that are substituted with *tert*-butyl, *iso*-propyl, and cyano groups are examined. These films are prepared by lifting the horizontal substrate through the air-water interface. The force-area data, Q-band spectra of the films, and *d*-spacing in powder X-ray diffraction patterns suggest that these phthalocyanines assume one-dimensionally assembled structures and edge-on configurations to the air-water interface. The dependence of the incident light angle on the Q-band absorption intensity in the phthalocyanine LB films, in polarized visible spectroscopy, supports that most of the phthalocyanine stacks exist as edge-on configurations to the air-water interface.

[6] The in-plane conductivities of undoped LB films of the Pc's containing cyano groups are measured. The film conductivity increases drastically by five orders of magnitude, when exposed to active gases such as iodine, triethylamine and *n*-butanethiol vapors. The conductivity responses to the gases are related to the estimated ionization potentials and electron affinities of the films.

[7] A previously reported divalent germanium phthalocyanine ($PcGe^{II}$) has been known to exhibit unusual electronic and mass spectra when compared with a corresponding high-valent germanium phthalocyanine. This is identified as μ-hydroxygermanium α,β,γ-triazatetrabenzcorrole ($TBC^{3-}Ge^{IV}OH$) from elemental analysis (C, H, N, Ge, and O), spectral measurement (EI- and FD-MS, visible, IR, and ^1H NMR), chemical reactivity, and oxidative titration results. This triazabenzcorrole ring is a new tetrapyrrolic macrocycle. TBC's containing Si, Al, and Ga have also been produced in a reaction mixture of $NaBH_4$. This type of metalloid Pc's ring contractive reaction is generally observed to occur with the

introduction of a reductive reagent such as $NaBH_4$ and H_2Se. The molecular symmetry of a TBCGe moiety is exactly C_1 or an approximately 2-fold symmetry showing some distortion. The serendipitous finding was initiated on the assumption that the divalent germanium phthalocyanine may form a one-dimensionally stacked phthalocyanine polymer incorporated with Ge-Ge spines.

ACKNOWLEDGEMENTS

I would like to express my sincerest gratitude to Professor Toyoki Kunitake, Department of Chemical Science and Technology, Faculty of Engineering, Kyushu University, for his continuous guidance and encouragement to represent this dissertation. I am also indebted to Professor Taku Matsuo, Professor Chisato Kajiyama, and Professor Hiroshi Taniguchi, Department of Chemical Science and Technology, Faculty of Engineering, Kyushu University, for their stimulating and advisory comments on the dissertation.

This work was carried out in Ibaraki Electrical Communication Laboratories, Nippon Telegraph and Telephone Corporation (NTT) from 1981 to 1988. I am especially indebted to Mr. Hisao Tabei for his sequential clue as a leader of the organic electric materials research project, where this work has been accomplished from 1982 to 1989. I am indebted to Mr. Yuzo Katayama (Tamura Co.), Mr. Kei Murase (NTT Advance Technology Co.) and Mr. Hiroaki Hiratsuka for their continuous guidance as research managers of the conducting organic materials research project from 1982 to 1987. I wish to thank Dr. Tatsuya Kimura, Mr. Hiroaki Hiratsuka, Dr. Tatsuo Izawa, and Dr. Nobuo Matsumoto, Basic Research Laboratories, NTT, for giving me an opportunity to write this work.

Grateful acknowledgment and thanks are made to all my collaborators, Dr. Fumihiro Ebisawa for his continuous and stimulating discussion on low-dimensional conducting materials, Dr. Saburo Imamura for his valuable discussion on electron beam resist properties of phthalocyanines containing alkylamides, Dr. Yuhei Mori for his advisory discussion on electronic structure of one-dimensional phthalocyanine conductors and assignment on the molecular structure of α,β,γ–triazatetrabenzcorrole, Mr. Takashi Kurihara for his valuable discussion on self-assembling features of phthalocyanines containing alkylamides and related organic compounds, and Mrs. Keiko Iimura-Shimada for her excellent technical assistance in evaluating electron beam resist properties. I wish to acknowledge to Associate Professor Kimio Isa, Department of Chemistry, Faculty of Education, Fukui University, for his triggering motivation and stimulating discussion during the study of α,β,γ–triazatetrabenzcorrole from its mass spectroscopy.

I acknowledge to Dr. Michio Sugi, Dr. Shin-ichi Kuroda, Dr. Kei-ichi Ikegami (Electrotechnical Laboratory), the rate Dr. Yasujiro Kawabata (National Chemical Laboratory for Industry) for their encouraging advices and discussion on the electrically conducting Langmuir-Blodgett films.

Finally, I want to thank my wife and children for their patience during the periods of time dedicated to this thesis.